SYNTHESIS OF DIGITAL FILTERS FROM FREQUENCY SPECTRUM CHARACTERISTICS

by

Arthur Laurent Partarrieu

United States
Naval Postgraduate School

THESIS

SYNTHESIS OF DIGITAL FILTERS
FROM FREQUENCY SPECTRUM CHARACTERISTICS

by

Arthur Laurent Partarrieu

September 1970

Synthesis of Digital Filters
from Frequency Spectrum Characteristics

by

Arthur Laurent Partarrieu
Teniente Segundo, Armada de Chile
Escuela Naval de Chile, 1964

Submitted in partial fulfillment of the
requirements for the degrees

MASTER OF SCIENCE IN ELECTRICAL ENGINEERING

and

ELECTRICAL ENGINEER

from the

NAVAL POSTGRADUATE SCHOOL
September 1970

ABSTRACT

A comparison of standard z transform and algebraic substitution synthesis methods for digital filters are presented with emphasis on the frequency domain characteristics. A generalization of Martin's procedure, which leads to recursive filters, is obtained. Also a new method to synthesize a digital filter from a magnitude squared versus frequency characteristic specification is presented.

TABLE OF CONTENTS

I. INTRODUCTION

Digital filters have become increasingly important because of technological developments in integrated circuits and digital techniques. This progress has increased the number of applications in which digital filtering techniques can be used. In spite of the fact that it is a relatively new development, a vast body of literature is available for digital filters. The relationship between digital filters and classical continuous filter theory can be depicted as in Fig. 1.1.

Start from the differential equation at the center of the diagram. The Laplace transform of the differential equation may be taken and a transfer function formed. The frequency spectrum of the continuous filter may be evaluated as shown in the diagram by letting $s = j\omega$. The upper part of the diagram shows the relationship between the transfer function of the continuous filter in the frequency domain, and the frequency domain characteristics of the sampled impulse response of the continuous filter. In deriving these results use is made of the Z transform. The lower part of the diagram shows numerical integration of the differential equations. Adopting a numerical integration algorithm yields a difference equation which can generally be expressed as a discrete time equation. For a given integration scheme, as illustrated in the diagram, it is possible to substitute a function of z (depending upon the type of integration) for the variable s

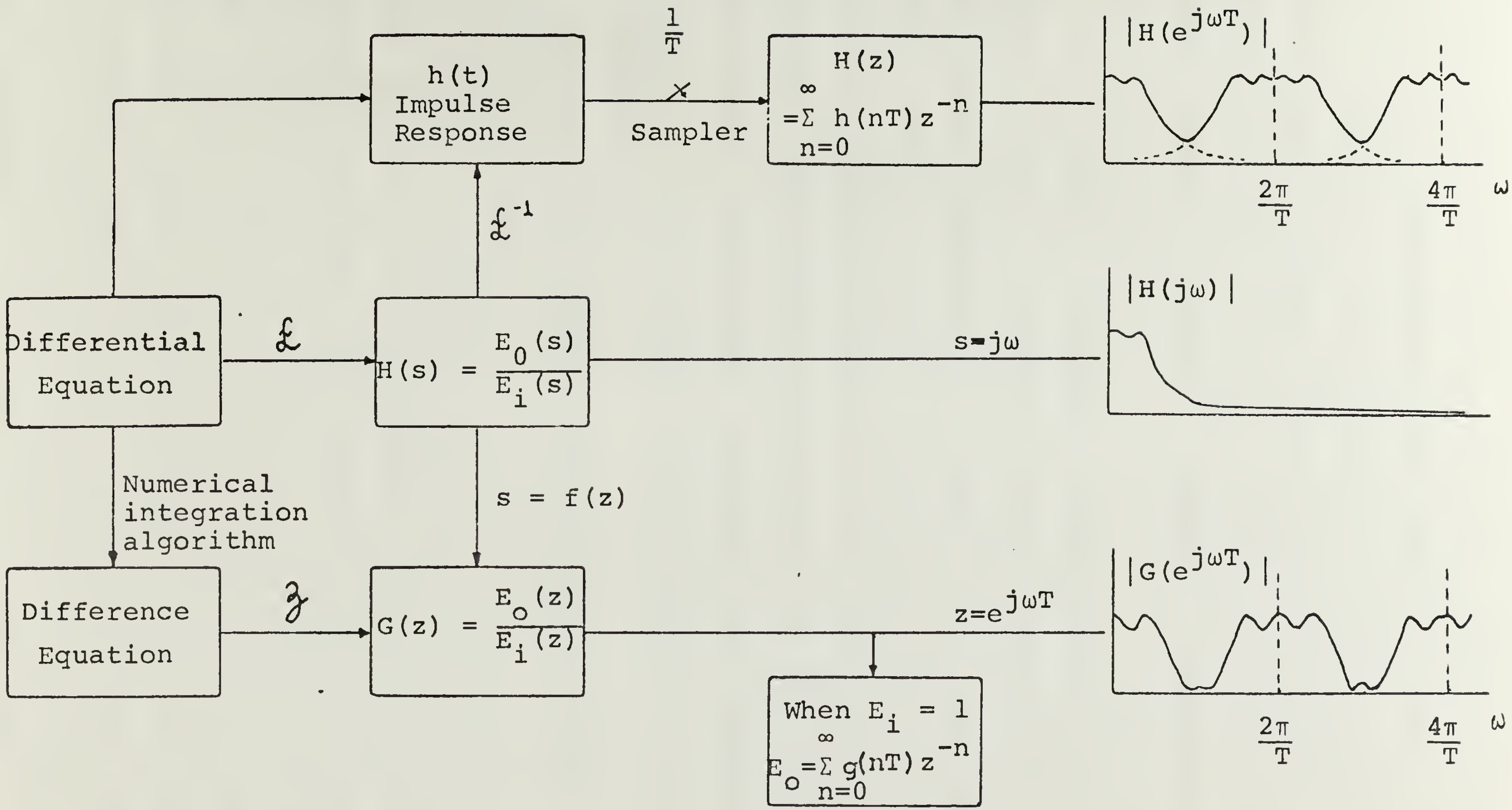

Fig. 1.1. Relationship between digital filter and continuous filter theory.

of the Laplace transformed continuous equation. When $z = \exp(j\omega t)$ is substituted in this equation a spectrum is obtained which, in general, is not identical to the spectrum of the sampled impulse response of the continuous filter. One of the objectives of this thesis is to compare numerical integration with the standard Z transform results as depicted in the upper portion of the diagram.

The Z transform technique is described in the work of J. Ragazzini and L. H. Zadah [1] and has been discussed by many other authors including B. C. Kuo [2]. J. Salzer [3] has written a classic paper on the comparison of digital integrators in the frequency domain with the ideal continuous integrator. The bilinear substitution, $s = \frac{2}{T}\frac{z-1}{z+1}$, which corresponds to trapezoidal integration, was considered very early by A. Tustin [4] and has been discussed thoroughly by K. Steiglitz [5].

In this thesis several areas of digital filter theory are considered in detail.

Chapter two contains a derivation of basic Z transform theory, a review of the synthesis of digital filters using standard Z transforms, and a discussion of the effect of sampling frequency on the frequency spectrum. The relationship between the s and z plane representation of the equations is presented. Chapter three contains a general interpretation of the algebraic substitution, $s = f(z)$, for several numerical integration techniques, a discussion of the bilinear substitution (trapezoidal integration), and a development of the effects of sampling time on the precision of numerical calculations.

Chapter four discusses the synthesis of digital filters from frequency spectrum characteristics. It contains a derivation, discussion, and a practical application of a direct method of synthesis originated by Martin [6]. A new generalization of this method to obtain recursive filters from a specification of magnitude versus frequency characteristics, is presented. The advantages of this technique include the fact that a zero phase shift filter can be obtained. Derivation of another new method of finding the coefficients of a digital filter, starting from a magnitude squared criterion, is presented. The advantages of this technique include reducing computer storage requirements, and reducing the number of multiplications to one half of those required by the Martin method. Chapter five presents a summary and several questions for future research.

II. THE Z TRANSFORM TECHNIQUE APPLIED TO DISCRETE TIME SIGNALS AND DIGITAL FILTERS

Systems may be classified as linear, time invariant, causal and so on. They may also be classified according to the nature of the signals present. A continuous signal is expressed as a continuous (or piecewise continuous) function of the independent variable, t. The signal must be uniquely defined at all values of t within a given range, except possibly at a denumerable set of points, as for example in a square wave. A discrete signal is defined only at a sequence of discrete values of the independent variable t. A quantized signal is one which can assume only a denumerable number of different values, but quantized signals may be either continuous or discrete, as discussed by P. M. DeRusso et al, [7].

There are many examples of continuous systems in nature, and they are to be found almost everywhere. Examples of discrete and quantized systems are perhaps more difficult to conceive but this does not mean they are scarce. For instance, the output of a continuous system when sampled for digital computation, or other purposes, becomes a discrete system. Some systems are discrete by nature. The distance to an object as measured with a pulsed radar; or a pulse coded communications system which is time multiplexed are examples of inherently discrete physical systems. A digital computer is an excellent example of a discrete, quantized system. The quantizing levels are determined ultimately by the finite number of bits of the

number representation. The discrete characteristic is determined by the fact that the independent variable assumes values at finite increments only.

In order to deal with discrete time quantized systems, existing Z transform theory has been extended [Ref. 2]. This theory was developed primarily for sampled data control systems and resembles Laplace transform theory for continuous systems in that it is operational in nature. The Z transform has proven to be useful for the study of all discrete time systems and it is extended approach which is reviewed in this chapter. Several important fundamentals are developed and a basic misapplication of the theory which occurs commonly in the literature, is discussed.

A. DEFINITION OF THE Z TRANSFORM OF A DISCRETE SIGNAL

Consider a continuous signal $x(t)$, for $t>0$, which is sampled at a frequency, f_s or equivalently, every $T = 1/f_s$ seconds.

Assume that the signal is sampled ideally, that is, the sampled signal assumes the value of the continuous signal with infinite accuracy at discrete values of the independent variable, $t = nT$; $n = 0,1,2, \ldots$

The process of sampling can be described as

$$x^*(t) = x(t)\ s(t) \tag{2.1}$$

where

$x^*(t)$ = the sampled signal

$x(t)$ = the continuous signal

$s(t)$ = the sampling function, representing a train of impulses, T seconds apart.

$$s(t) = \sum_{n=0}^{\infty} \delta\ (t-nT) \tag{2.2}$$

From (2.1) and (2.2)

$$x^*(t) = \sum_{n=0}^{\infty} x(nT)\ \delta\ (t-nT) \tag{2.3}$$

Taking the Laplace transform of the sampled signal we have from Eq. (2.3)

$$\begin{aligned} X^*(s) &= \mathcal{L}\{x^*(t)\} \\ &= \sum_{n=0}^{\infty} x(nT)\ \mathcal{L}\{\delta(t-nT)\} \end{aligned} \tag{2.4}$$

But $\mathcal{L}\{\delta(t-nT)\} = e^{-nTs}$ (2.5)

so that Eq. (2.4) becomes

$$X^*(s) = \sum_{n=0}^{\infty} x(nT)\ e^{-nTs} \tag{2.6}$$

Now, define a new variable z, such that

$$z = e^{sT} \tag{2.7}$$

so that Eq. (2.6) becomes

$$X(z) = X^*(s)\Big|_{z=e^{sT}} = \sum_{n=0}^{\infty} x(nT)\ z^{-n} \tag{2.8}$$

The standard procedure to find the Z transform of a discrete signal can be summarized as follows:

(a) Sample the continuous signal

(b) Find the Laplace transform of the sampled function

(c) Substitute $e^{sT} = z$ in the Laplace transform of the sampled signal to obtain the Z transform.

Using common notation, the above can be written as follows:

$$X(z) = \mathcal{Z}\{x(t)\} = [\mathcal{L}\{x^*(t)\}]\Big|_{z=e^{sT}} \tag{2.9}$$

This process of obtaining the Z transform of a signal is illustrated in Fig. 2.1.

1. Obtaining the Z Transform in Closed Form

The foregoing definition of the Z transform provides a method for obtaining the transform of a signal, but it has two disadvantages:

a. Results are presented in open form because the transform of a signal is given as a summation of inverse powers of z whose coefficients are the values of the signal at the sampling times. For sampled functions derived from continuous functions with poles in the left half s plane, such coefficients will eventually decay to zero. If the decaying process is slow compared to the sampling interval, a large number of terms in the sampled Z transform expansion are required to represent the successive values.

b. The process of obtaining the Z transform may be very long, particularly when only the Laplace transform of the continuous signal is known. The process requires taking the inverse Laplace transform of the continuous signal, sampling

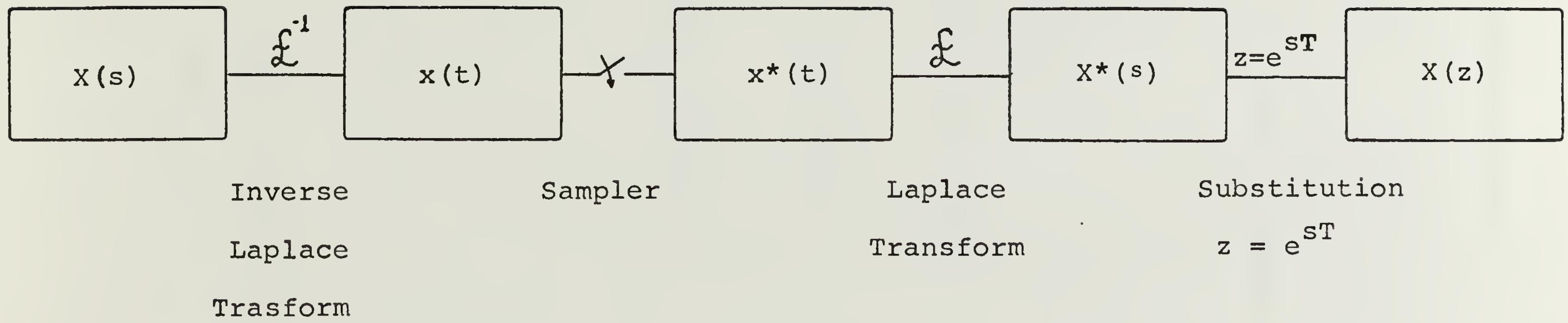

Fig. 2.1. Procedure to obtain the z Transform

the resulting time function, and finally expressing the sample values as a series of inverse powers of z.

There is an alternate method for obtaining the Z transform of a signal that is particularly suitable when the Laplace transform of the continuous signal is known. This latter approach gives the result in closed form. From Eq. (2.1)

$$X^*(s) = \mathcal{L}\{x(t)\ s(t)\} \tag{2.10}$$

and so $$X^*(s) = X(s) * S(s) \tag{2.11}$$

where the asterisk denotes convolution.

$$X^*(s) = \frac{1}{2\pi j}\int_{c-j\infty}^{c+j\infty} X(\lambda)\ S(s-\lambda)\ d\lambda \tag{2.12}$$

now $$S(s) = \int_0^\infty \sum_{n=0}^{\infty} \delta\ (t-nT)\ e^{-st}\ dt$$

$$S(s) = \sum_{n=0}^{\infty} e^{-nTs}$$

$$S(s) = 1 / (1-\exp(-sT)) \tag{2.13}$$

provided $|\exp(-nT)| < 1$

In (2.11), use has been made of the sifting integral property of the impulse, namely

$$\int_0^\infty \delta\ (t-nT)\ f(t)\ dt = f(nT) \tag{2.14}$$

Therefore, the Laplace transform of the sampled function can be written in terms of the complex convolution integral

$$X^*(s) = \frac{1}{2\pi j} \int_{c-j\infty}^{c+j\infty} X(\lambda) \frac{1}{1-e^{-(s-\lambda)T}} \, d\lambda \tag{2.15}$$

If Γ_1 as shown in Fig. 2.2 is taken as the path enclosing the left half of the s plane then integral (2.15) may be divided into two integrals as follows

$$X^*(s) = \frac{1}{2\pi j} \oint_{\Gamma_1} X(\lambda) \frac{1}{1-e^{-(s-\lambda)}} \, d\lambda$$

$$- \frac{1}{2\pi j} \oint X(\lambda) \frac{1}{1-e^{-(s-\lambda)}} \, d\lambda \tag{2.16}$$

Note that Γ_1 is composed of the straight line joining the points $(c,-j\infty)$ and $(c,+j\infty)$ and the counter-clockwise semi-circle or infinite radius.

If the condition

$$\lim_{s \to \infty} s\,X(s) = 0 \tag{2.17}$$

is met, then the second integral tends towards zero and Eq. (2.16) becomes

$$X^*(s) = \frac{1}{2\pi j} \oint_{\Gamma_1} X(\lambda) \frac{1}{1-e^{-(s-\lambda)}} \, d\lambda \tag{2.18}$$

A very important case occurs when the Laplace transform X(s) of the continuous signal is a ratio of two

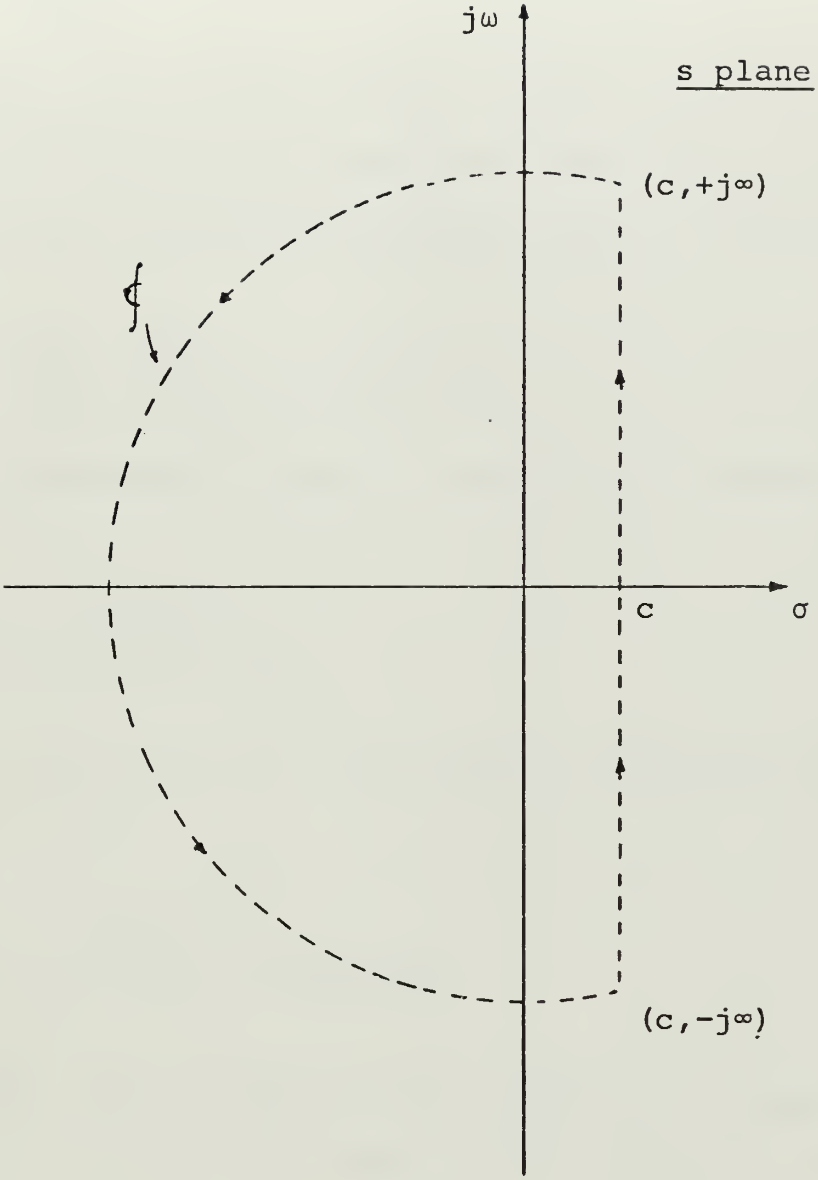

Fig. 2.2. The contour integration path Γ_1.

two polynomials

$$X(s) = \frac{N(s)}{D(s)} \tag{2.19}$$

In this case the function, X(s), has a finite number of poles and the integral around the closed path can be evaluated using the residue theorem. Thus Eq. (2.18) becomes

$$X^*(s) = \sum_{n=1}^{k} \frac{N(\lambda_n)}{D'(\lambda_n)} \frac{1}{1- e^{-(s-\lambda_n)T}} \tag{2.20}$$

where k is the number of simple poles of $X(\lambda)$ located at λ_n, with

$$D'(\lambda_n) = \left.\frac{d\, D(s)}{ds}\right|_{s=\lambda_n} \tag{2.21}$$

and substituting Eq. (2.7) into (2.20), yields X(z) the Z transform of x(t)

$$X(z) = \sum_{n=1}^{k} \frac{N(\lambda_n)}{D'(\lambda_n)} \frac{1}{1- e^{\lambda_n T} z^{-1}} \tag{2.22}$$

The above formula (2.22) represents a closed form for the Z transform of the signal which contains as many terms as the degree of the denominator polynomial of the function X(s). Expansion of Eq. (2.22) in a series of inverse powers of z yields Eq. (2.8).

B. SYNTHESIZING A DIGITAL FILTER WITH THE STANDARD Z TRANSFORM

In the previous section two methods have been developed to obtain the Z transform of a sampled signal, starting from either the continuous time function or its Laplace transform.

The same procedure can be followed to obtain the Z transform corresponding to the sampled output of a continuous filter, considering the signal to be the impulse response of the filter, $h(t)$.

In general there are many known procedures for the design of continuous filters to meet various types of specifications. These procedures are usually described in the s domain or in the frequency domain, $s = j\omega$. The Z transform is used to translate continuous time realizations into discrete time realizations or digital filters.

In control theory, when the differential equations of the systems are known, it is often necessary to simulate continuous systems on a digital computer. One approach is to consider the impulse response which is the inverse Laplace transform of the system's transfer function. The Z transform can be applied to this signal after sampling, yielding a discrete simulation of the system.

Equation (2.8) assures that the Z transform of a digital filter or system, when expanded in terms of inverse powers of z, represents identically the impulse response of the continuous filter or system sampled at intervals T.

If $X(z)$ is the Z transform of the input signal to a system, and if $H(z)$ is the Z transform of the system transfer junction, then

$$Y(z) = X(z)\, H(z) \tag{2.23}$$

Here Y(z) represents the Z transform of the output signal, and corresponds to the numerical convolution of the input signal an the system transfer function, as is demonstrated below.

$$X(z) = \sum_{m=0}^{\infty} x(mT)\ z^{-m}$$

$$H(z) = \sum_{k=0}^{\infty} h(kT)\ z^{-k} \qquad (2.24)$$

where h(kT) is the sampled impulse response of the system.

Substituting (2.24) into (2.23)

$$Y(z) = \sum_{m=0}^{\infty} \sum_{k=0}^{\infty} x(mT)\ h(kT)\ z^{-(k+m)} \qquad (2.25)$$

and replacing subscripts, such that $k+m = n$ or $k = n-m$, then the limits of the summations are converted as follows: $k = 0$ becomes $n = m$ and $k = \infty$ becomes $n = \infty$.

Thus (2.25) becomes

$$Y(z) = \sum_{m=0}^{\infty} \sum_{n=m}^{\infty} x(mT)\ h((n-m)T)\ z^{-n} \qquad (2.26)$$

Changing the order of the summations and neglecting or adding zero terms of the type h(-kT) (k=1,2,.....) yields

$$Y(z) = \sum_{n=0}^{\infty} \sum_{m=0}^{n} X(mT)\ h((n-m)T)\ z^{-n} \qquad (2.27)$$

$$= \sum_{n=0}^{\infty} y(nT)\ z^{-n}$$

Hence the coefficient $y(nT)$ of z^{-n} in $Y(Z)$ is given by

$$y(nT) = \sum_{m=0}^{n} x(nT)\, h((n-m)T) \tag{2.28}$$

Equation (2.28) is the numerical convolution of the input samples and the digital filter sampled impulse response.

The output signal transform, $Y(z)$, when expanded in a series of inverse powers of z represents the output signal at different times. If $X(z)$ and $H(z)$ are obtained from sampling a continuous input signal and the impulse response of a continuous system or filter respectively, then the coefficients in the expansion of $Y(z)$ will correspond to the sampled output of the continuous system or filter. Hence when synthesizing a digital filter using the Z transform of a continuous filter impulse response sampled at intervals T, the resulting output signal is an exact description in the time domain in the sense that the output values of the digital realization will be equal to the values of the continuous filter output signal sampled at intervals T.

Regarding the frequency spectrum of the filters, consider a continuous system with transfer function $H(s)$. If an input signal $E_i(s)$ is applied, the output signal $E_o(s)$ has a Laplace transform

$$E_o(s) = H(s)\, E_i(s) \tag{2.29}$$

The inverse Laplace transform of $E_o(s)$ is the output signal $e_o(t) = \mathcal{L}^{-1}\{E_o(s)\}$, which now is sampled at the rate of 1 / T samples per second, yielding the sampled output signal

$e_o*(t)$ as shown in Fig. 2.3a. The Fourier transform of this signal is the desired output spectrum

$$E_o*(j\omega) = \mathfrak{F}\{e_o*(t)\} \qquad (2.30)$$

This spectrum could also have been obtained by convolving the Fourier transform of the sampling function $\sum_{n=-\infty}^{\infty} \delta[j(\omega - n\omega_s)]$ such that

$$E_o*(j\omega) = E_o(j\omega) * \sum_{n=-\infty}^{\infty} \delta[j(\omega-n\omega_s)] \qquad (2.31)$$

$$= \sum_{n=-\infty}^{\infty} E_o(j[\omega-n\omega_s])$$

This signal processing may be compared with the development of the digital filter shown in Fig. 2.3b. We assume the same sampling frequency $f_s = 1 / T$ and obtain the Z transform $H(z)$ of the filter function $H(s)$. Then the Z transform of the filter output $E_o(z)$ is given by

$$E_o(z) = H(z)\, E_i(z) \qquad (2.32)$$

where $E_i(z)$ is the Z transform of the sampled filter input $e_i*(t)$. Substituting $z = \exp(j\omega T)$ into $E_o(z)$ yields the desired output spectrum $E_o*(j\omega)$. The following question may now be asked: Is this output spectrum of the digital filter identical with the output spectrum obtained in Eq. (2.31)? This question is discussed in the next section.

1. <u>The Effect of Sampling on the Frequency Spectrum</u>

For a signal of finite bandwidth w radians called a band limited signal shown in Fig. 2.4a Shannon's Sampling

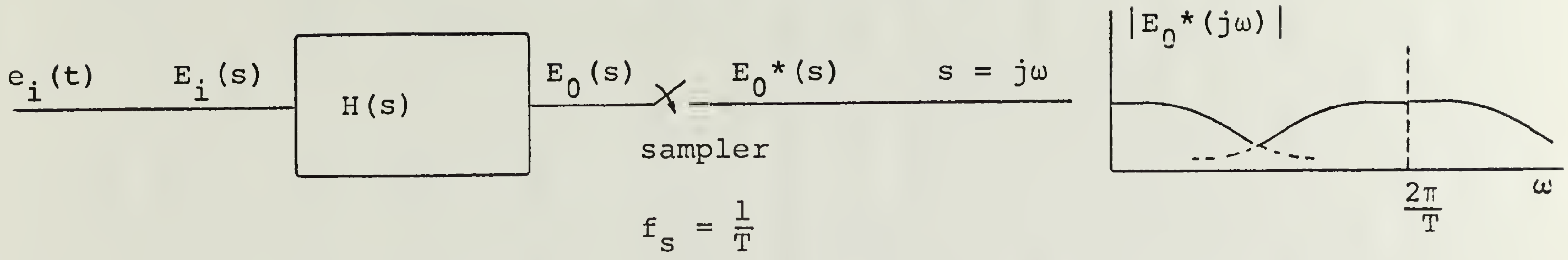

(a) Continuous filter with sampler.

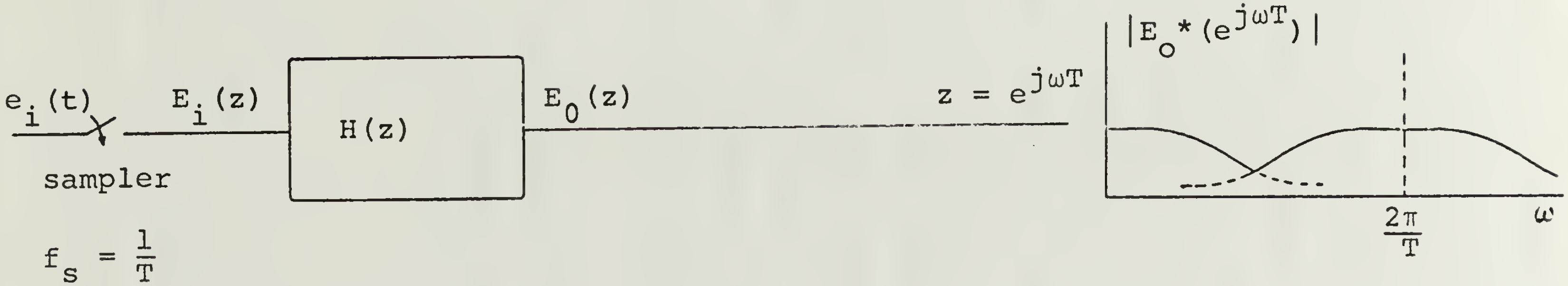

(b) Equivalent discrete filter

Fig. 2.3. Equivalence between discrete and continuous filters at sampling instants.

Theorem [8], requires a sampling rate equal to at least twice the maximum frequency w of the signal in order to recover the signal without distortition after passing it through an ideal low pass filter. The spectrum of the signal sampled at a higher rate than the Nyquist rate is shown in Fig. 2.4b. If the sampling frequency is lower than the limit set by Nyquist, then some overlapping of spectrum will occur. This is known as the aliasing effect and is illustrated in Fig. 2.4c. It has been shown by L. J. Fogel [9], that it is possible to recover a signal sampled at a lower rate than Nyquist (or one for which aliasing has taken place) if for every sample additional information about the signal is known. For example, this is possible if its derivatives with respect to time are known. However, this idea cannot be applied here because we restrict ourselves to single input filters where only the values of the signal are known.

To answer the previous question regarding comparison of the two spectra of Fig. 2.3, consider the continuous case of Fig. 2.3a, where for $s = j\omega$

$$E_o(j\omega) = H(j\omega)\ E_i(j\omega) \tag{2.33}$$

After sampling this spectrum, $E_o{}^*(j\omega)$ is the convolution of $E_o(j\omega)$ and the spectrum of the sampling signal, which is a train of impulses separated by ω_s on the ω axis as given by Eq. (2.31). The effect is to make the sampled spectrum repetitive with period ω_s. From Shannon's Sampling Theorem, the sampled output can be reconstructed without aliasing distortion provided $E_o(j\omega)$ is band limited and the sampling frequency

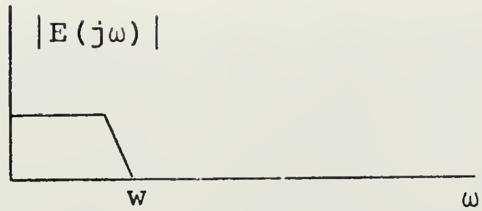

(a) Spectrum of a band limited signal

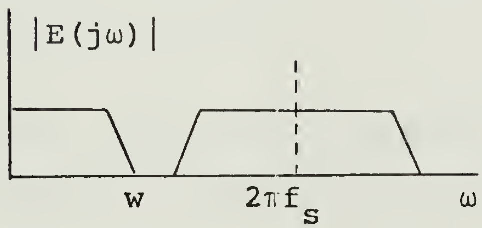

(b) Spectrum of a sampled band limited signal, $f_s > 2w$

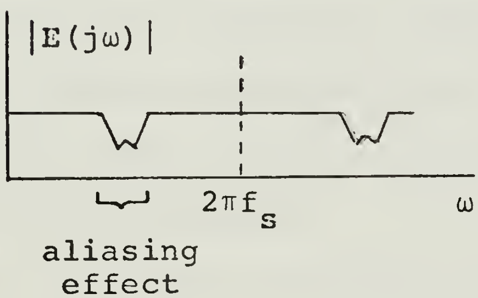

(c) Spectrum of a sampled band limited signal, $2\pi f_s < 2w$

Fig. 2.4. Effect of sampling frequency on the frequency spectrum of the sampled signal.

is higher than two times the maximum frequency of $E_o(j\omega)$. For $E_o(j\omega)$ to be band limited either $E_i(j\omega)$ or $H(j\omega)$ have to be band limited.

Consider now the discrete case shown in Fig. 2.3b, where $e_i(t)$ is sampled and the Z transform is obtained. From Eq. (2.8)

$$E_i(z) = E_i^*(s)\Big|_{z = e^{sT}} \tag{2.34}$$

Substituting Eq. (2.34) into equation (2.32) yields

$$E_o^*(e^{j\omega T}) = H^*(e^{j\omega T})\ E_i^*(e^{j\omega T}) \tag{2.35}$$

As may be seen, the output spectrum $E_o^*(e^{j\omega T})$ is the product of the two spectra $H^*(e^{j\omega T})$ and $E_i^*(e^{j\omega T})$. Clearly both these spectra must be undistorted (no aliasing) if $E_o^*(e^{j\omega T})$ is to be undistorted. Hence for this case the requirement is different from the case of Fig. 2.3a. In view of the above remarks we conclude that it is necessary to have $E_i(j\omega)$ and $H(j\omega)$ band limited and furthermore, one must sample at a frequency above the Nyquist rate for both spectra of Figs. 2.3a and 2.3b to be identical.

As an example consider the design of a digital low pass filter with a cut off frequency of 2 KHz which is required to filter a signal of 10 kHz bandwidth. Such a filter must be designed with a sampling rate greater than 20 kHz. Note that if the signal had been obtained from a continuous filter, it could be recovered by sampling at a rate of only 4 kHz.

It is clear from the above remarks and the example given, that there is a maximum frequency that can be handled by a

digital filter in real time operation. In fact this limit will depend on the computing speed of the processor and the general complexity of the filter. It is desirable to keep digital filter designs as simple as possible, although considerations of stability may modify these considerations.

2. The Interelationship Between the s and z Planes

The interelationship between the s plane and the z plane can be derived from the definition of the variable z namely

$$z = e^{sT} \tag{2.36}$$

A point in the s plane, namely $(\sigma+j\omega)$ will be mapped into the point in the z plane

$$z = e^{(\sigma+j\omega)T} = e^{\sigma T} e^{j\omega T} \tag{2.37}$$

and so $|z| = e^{\sigma T}$

Therefore, the points in the s plane with constant damping, i.e., σ = constant, map onto a circle of constant radius, $e^{\sigma T}$, in the z plane. Points in the s plane with constant frequency, i.e. ω = constant, map onto radial lines, $\arg z = \omega T$.

Furthermore, for points in the left half s plane $\sigma < 0$, and so

$$|z| = e^{\sigma T} < 1 \quad \text{for} \quad T > 0 \tag{2.38}$$

Equation (2.38) indicates that the entire L.H.P. maps into the inside of the unit circle in the z plane.

Although useful, the foregoing discussion may be misleading unless it is applied properly. The misuse of Eq. (2.36) occurs often in the literature. Take for example the paper by C. J. Greaves and J. A. Cadzow [10]. Their mistake consists of replacing the variable s in the Laplace transform of the continuous filter by its corresponding z, with $s = (1/T) \ln z$ as

$$H(z) = H(s)\Big|_{s = (1/T)\ln z} \tag{2.39a}$$

This equation is in error and should be replaced by

$$H(z) = H^*(s)\Big|_{s = (1/T)\ln z} \tag{2.39b}$$

The reason is clear from the closed form expression for the Z transform, Eq. (2.18), where before the substitution of variables is made, a complex integral has to be evaluated.

However, there is a direct connection between the Laplace transform of the continuous function and the Z transform of the sampled function. Namely the poles of the Laplace transform of the continuous function are mapped into the z plane of the sampled function using the mapping function of (2.36).

This can be seen from equation (2.22) where every term in the summation will have a pole in the z plane at

$$z = e^{\lambda_n T} \tag{2.39c}$$

which indicates the mapping of the singularity λ_n according to the mapping relation of (2.36).

In summary Eq. (2.36) may only be used to transform poles of the continuous function in the s plane to pole locations of the sampled function in the z plane. It does not represent a change in variable except when applied directly to a sampled signal. As noted this subtlety has proven to be a source of many mistatements in the literature.

III. THE ALGEBRAIC SUBSTITUTION METHOD

An equivalent digital representation of a continuous system or filter is often required in practice. This could arise, for example, in a digital simulation of a continuous control problem, or in an attempt to extend continuous filter theory to provide digital filter realizations. This latter application is very appealing because continuous filter theory is very well developed and procedures exist to match given specifications to filter relizations. Designs have been tabulated and are available in many handbooks. If a direct method to obtain the equivalent digital realization of a continuous filter exists, it would make all previous knowledge of continuous filter theory available for the discrete case.

It is convenient when implementing a digital filter, to obtain its representation as a Z transform, and particularly as a ratio of two polynomials of inverse powers of z. Such a representation indicates the linear combinations which have to be performed upon past values of input and output signals samples, to obtain the present value of the output.

The most common description of continuous filters in the s domain is as a ratio of two polynomials in s and so it is convenient to have a rational function of z to directly replace for s in the continuous type description. This is if

$$s = f(z) \tag{3.1}$$

then $H(s) = H(f(z)) = G(z)$. (3.2)

If the function f(z) is a ratio of two polynomials of inverse powers of z and if H(s) is a ratio of two polynomials in s, then G(z) in Eq. (3.2) is assured to be the ratio of two polynomials in inverse powers of z.

This procedure, described in Eq. (3.2) is called the algebraic substitution technique, and converts rational polynomials in s into the desired rational polynomials in z.

It will be shown that the selection of a specific f(z) to substitute for s, corresponds to the adoption of a numerical integration algorithm to integrate the phase state variables of the filter or system in discrete time.

A. MEANING OF THE ALGEBRAIC SUBSTITUTION s = f(z)

In order to find functions that can replace the variable s in the description of the continuous filter, H(s), the meaning of the substitution must be understood. In the first place, the variable s of the Laplace transform theory represents an operator in the time domain, i.e., it is a differentiator. Similarly, the inverse of s, s^{-1}, represents an integrator.

Consider a filter whose transfer function is

$$H(s) = \frac{a_o + a_1 s + \dots + a_n s^n}{b_o + b_1 s + \dots + b_m s^m}, \text{ where } m \geq n \tag{3.3}$$

If this transfer function is the ratio of the output signal transform to the input signal transform with zero initial conditions, then Eq. (3.3) can be expanded as follows

$$H(s) = \frac{Y(s)}{X(s)} = \frac{W(s)}{X(s)} \cdot \frac{Y(s)}{W(s)} \tag{3.4}$$

The following equations can be formed arbitrarily

$$\frac{W(s)}{X(s)} = \frac{1}{b_o + b_1 s + b_2 s^2 + \ldots + b_m s^m} \qquad (3.5)$$

$$\frac{Y(s)}{W(s)} = a_o + a_1 s + \ldots + a_n s^n \qquad (3.6)$$

Rearranging Eq. (3.5) and (3.6) yields

$$b_m s^m W(s) = X(s) - \sum_{j=0}^{m-1} b_j s^j W(s) \qquad (3.7)$$

$$Y(s) = \sum_{j=0}^{n} a_j s^j W(s) \qquad (3.8)$$

Equations (3.7) and (3.8) can be illustrated as in Fig. 3.1, indicating a possible implementation, as is usually done in an analog computer simulation for low order systems.

It has been shown that a transfer function of the type described in Eq. (3.3), can always be expanded in the form shown in Fig. 3.1. From this illustration it can be seen, that the replacement of the integrations (denoted by 1/s in the state space expansion of a continuous filter) by a function of z, 1/f(z), corresponds to a direct algebraic substitution of the variable s by the function s = f(z) in the closed form expression of Eq. (3.3).

Furthermore, the linear operation 1/f(z), should perform an approximate operation in the discrete time domain similar to the operation, 1/s, of the transform domain, if the responses obtained with the digital filter are to resemble the responses obtained from the continuous system.

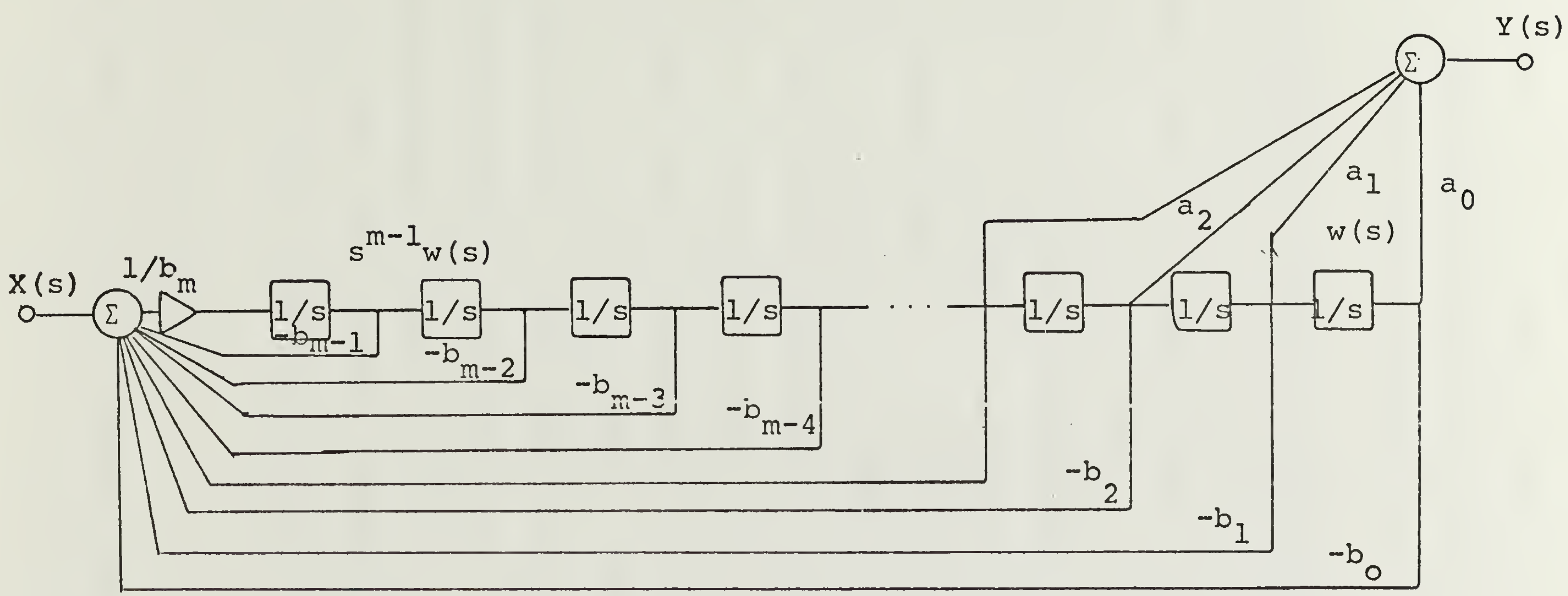

Fig. 3.1. State Space expansion of a Transfer Function.

In view of the above remarks, it can be concluded that the algebraic substitution technique represents the adoption of a numerical integration algorithm to perform the operation of integration for the state variables of the filter.

B. OBTAINING RECURSIVE INTEGRATION ALGORITHMS

To derive recursive integration algorithms, it must be decided whether or not the present value of the input is available to compute the present value of the output. This question can be settled if some assumptions are made. For instance, if the time required to perform the computations is considered negligible, that is if the time elapsed between the present input and the corresponding output of the filter is of no importance, then the algorithms can be derived using interpolation formulas. On the other hand, when this factor is considered important and the output at the present time is computed without the present input value, then some extrapolation formula must be used. This latter condition involves some form of a predicting method, and intuitively seems to be less accurate. Among several different criteria to find recursive integration algorithms, the following methods are described because they lead to well known integration formulas which are used in practice.

a. The Adams-Moulton Method.

This method is derived from the expression

$$y_k = y_{k-1} + \int_{t_{k-1}}^{t_k} f_x(t)\, dt \tag{3.9}$$

where $f_x(t)$ is a polynomial of $(n-1)^{-st}$ degree approximating the input signal, based on the last n available input values.

The recursive integration algorithms for the first two degrees of approximating polynomials are

n	Interpolating Form (Using last input)	Extrapolating Form (Not using last input)
1	$y_k = y_{k-1} + \frac{T}{2}(X_k + X_{k-1})$	$y_k = y_{k-1} + \frac{T}{2}(3X_{k-1} - X_{k-2})$
2	$y_k = y_{k-1} + \frac{T}{12}(5X_k + 8X_{k-1} - X_{k-2})$	$y_k = y_{k-1} + \frac{T}{12}(23X_{k-1} - 16X_{k-2} + 5X_{k-3})$

From these algorithms it can be seen that the first degree approximation using the last input value is the well known Trapezoidal rule of integration.

b. The Milne's Method.

This method correspond to the numerical integration criterion

$$y_k = y_{k-n} + \int_{t_{k-n}}^{t_k} f_x(t)\, dt \tag{3.10}$$

where $f_x(t)$ is the polynomial of $(n-1)^{-st}$ degree approximating the input function using the last n available values of the inputs.

Clearly, when the approximating degree n is unity Adams-Moulton and Milne's methods are the same, giving identical recursive integration algorithms. For a polynomial approximation of second degree the recursive Milne's algorithms are:

n	Interpolating Form (Using last input)	Extrapolating Form (Not using last input)
2	$y_k=y_{k-2}+\frac{T}{3}(X_k+4X_{k-1}+X_{k-2})$	$y_k=y_{k-3}+\frac{4T}{3}(2X_{k-1}-X_{k-2}+2X_{k-3})$

It can be seen that Milne's first degree formula also leads to the trapezoidal rule and that the second degree formula leads to the Simpson's 1/3 rule of integration, when the last input is used.

These recursive integration algorithms as well as others have been analyzed in the literature under the general category of digital integrators, as for example in one of the first papers on the subject which was published by John M. Salzer in 1953 [3], or in a paper by A. P. Sage and R. W. Burt [11].

To obtain the frequency spectra of the algorithms, one must first obtain the equivalent Z transform representation. For example consider the trapezoidal rule of integration

$$y_k = y_{k-1} + \frac{T}{2} (X_k + X_{k-1}) \tag{3.11}$$

The equivalent digital filter can be derived by taking the Z transform

$$Y(z) = z^{-1} Y(z) + \frac{T}{2} (X(z) + z^{-1} X(z)) \tag{3.12}$$

and the filter transfer function is

$$H(z) = \frac{Y(z)}{X(z)} = \frac{T}{2} \frac{1 + z^{-1}}{1 - z^{-1}} \tag{3.13}$$

This function corresponds to the algebraic substitution

$$s \Leftrightarrow \frac{2}{T} \frac{1 - z^{-1}}{1 + z^{-1}} \tag{3.14}$$

The frequency spectrum of the filter described in (3.13) is obtained by substituting $z = \exp(j\omega T)$

$$H(e^{j\omega T}) = (\frac{T}{2}) \frac{1 + e^{-j\omega T}}{1 - e^{-j\omega T}} \tag{3.15}$$

$$H(e^{j\omega T}) = -j \frac{T}{2} \text{cotan} \frac{\omega T}{2} \tag{3.16}$$

and hence

$$|H(e^{j\omega T})| = \text{cotan} \frac{\omega T}{2} \tag{3.17}$$

$$\text{Arg } H(e^{j\omega T}) = - \frac{\pi}{2} \tag{3.18}$$

These equations can be compared with the magnitude and phase of an ideal integrator

$$H(s) = \frac{1}{s} \tag{3.19}$$

$$H(j\omega) = \frac{1}{j\omega} \tag{3.20}$$

$$|H(j\omega)| = \frac{1}{\omega} \tag{3.21}$$

$$\text{Arg } H(j\omega) = -\frac{\pi}{2} \tag{3.22}$$

Equation (3.17) can be expanded in a series of the form

$$|H(e^{j\omega T})| = \frac{T}{2} \left(\frac{2}{\omega T} - \frac{\omega T}{6} - \frac{\omega^3 T^3}{360} - \ldots\right) \simeq \frac{1}{\omega} - \frac{\omega T^2}{12} \tag{3.23}$$

and therefore the magnitude spectrum of the trapezoidal rule digital integrator approximates the magnitude of an ideal integrator for values of ω such that

$$\frac{\omega T^2}{12} << \frac{1}{\omega} \tag{3.24}$$

or equivalently

$$\omega << \frac{\sqrt{12}}{T} \tag{3.25}$$

or

$$\omega << \frac{\sqrt{3}}{\pi} \omega_s \simeq \frac{1}{2} \omega_s \tag{3.26}$$

In Salzer's paper a study of the frequency spectra of several different digital integrators is considered with a comparison to the spectrum of an ideal integrator.

Figure 3.2 shows curves of the trapezoidal rule and Simpson's 1/3 rd rule plotted against $\Omega = \omega/\omega_s$. The straight line or real axis represents the ideal integrator and as can be seen the trapezoidal rule falls below this line, while Simpson's rule lies above this line.

In general it can be said that the more complex the integration algorithm, the wider the band of coincidence with the ideal integrator and also the larger the number of multiplications to be performed or the increase in computation time. As a result a possible figure of merit might be the ratio of 3 db bandwidth to the number of multiplications. As a matter of fact, simpler integration schemes perform as well or better than the complex ones in terms of the above figure of merit.

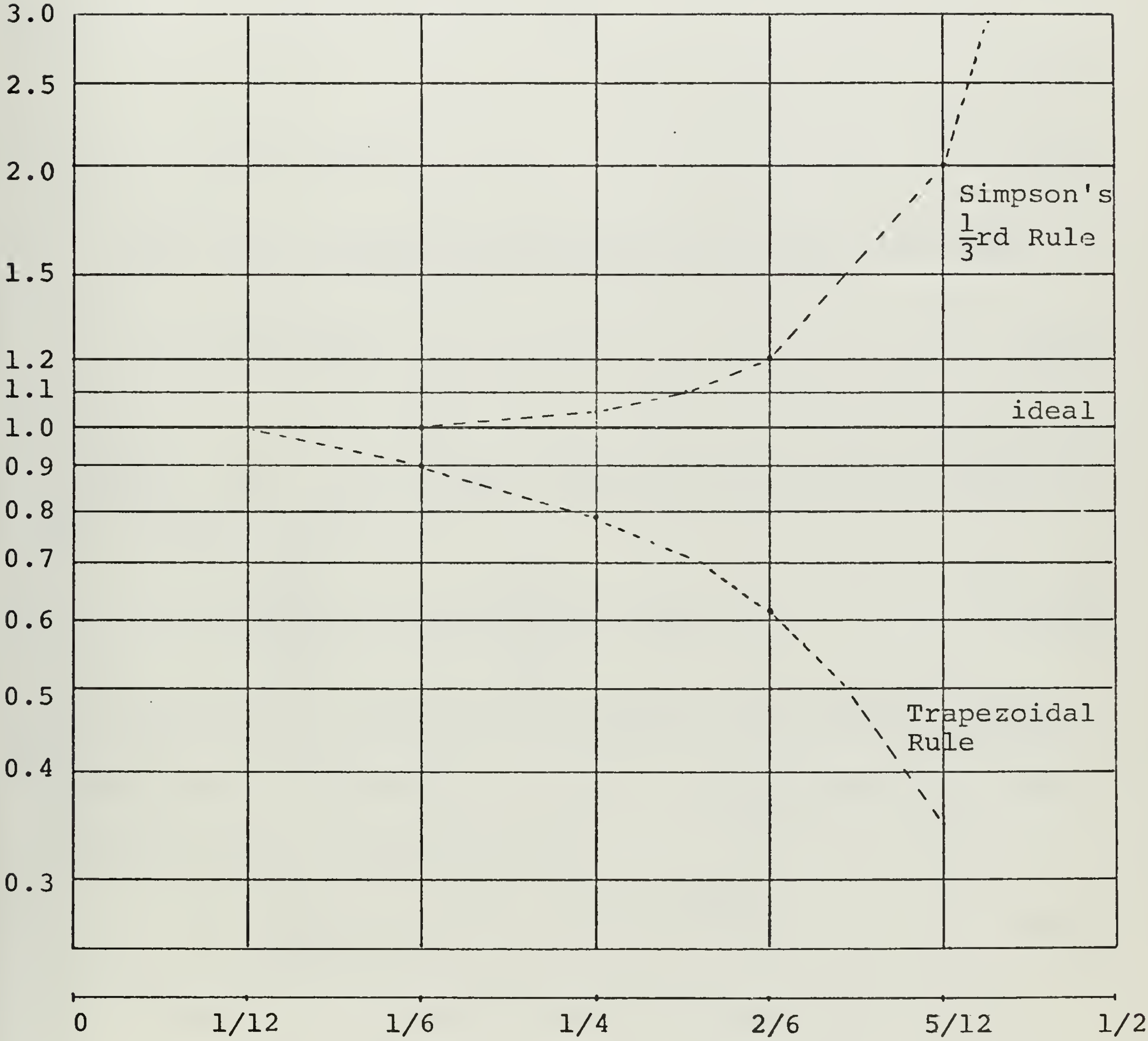

Fig. 3.2. Digital Integrators comparison with ideal continuous Integrator, as function of normalized frequency.

C. THE BILINEAR SUBSTITUTION

This particular case of the algebraic substitution technique corresponding to the adoption of the trapezoidal rule of integration has a different interpretation, as is shown by K. Steiglitz [5], and also discussed by Gold and Rader [15].

In order to avoid confusion between variables, the following notation will be used:

$$s = \sigma + j\omega \tag{3.27}$$

$$z = e^{(\delta + j\Omega)T} \tag{3.28}$$

When the bilinear transformation is made, such that

$$s = \left(\frac{2}{T}\right) \frac{z - 1}{z + 1} \tag{3.29}$$

then the entire $j\omega$ axis is mapped onto the unit circle in the z plane. This can be shown from the inverse relationship of Eq. (3.29), namely

$$z = \frac{1 + \left(\frac{T}{2}\right) s}{1 - \left(\frac{T}{2}\right) s} = \frac{1 + \left(\frac{T}{2}\right) j\omega}{1 - \left(\frac{T}{2}\right) j\omega} \Rightarrow |z| = 1 \tag{3.30}$$

To find the relationship between the variable ω in the s plane and the variable Ω in the z plane when $s = j\omega$, the following equation may be used

$$z = \frac{1 + \left(\frac{T}{2}\right) j\omega}{1 - \left(\frac{T}{2}\right) j\omega} = e^{j\Omega T} = e^{j2 \tan^{-1} \frac{\omega T}{2}} \tag{3.31}$$

Equation (3.31) may be reduced to the form

$$\Omega = \frac{2}{T} \text{arc tan} \frac{\omega T}{2} \tag{3.32}$$

Equation (3.32) indicates the transformation relating the frequency axis of the s and z planes. Equation (3.29) means that when the bilinear transformation is applied to a rational expression in powers of s, H(s), a rational expression G(z) in powers of z is obtained.

$$G(z) = H\left(\frac{2}{T}\,\frac{z - 1}{z + 1}\right) \tag{3.33}$$

Furthermore, when the frequency spectrum of the s domain representation is obtained by evaluating the expression H(s) when $s = j\omega$, and $H(j\omega)$ is obtained, and similarly if the frequency spectrum of the expression in powers of z is evaluated along the unit circle, the function obtained is

$$G(e^{j\Omega T}) = H\left(\frac{2}{T}\ \text{arc tan}\ \frac{\omega T}{2}\right) \tag{3.34}$$

The resulting function has the same spectrum as $H(j\omega)$ but compressed into the interval $-\pi/T \leq \Omega \leq \pi/T$.

The nonlinearity of the frequency scale can be overcome by prewarping [Ref. 15] or frequency scaling the chosen continuous realization, such that after the transformation the selected frequency is at the desired value. However, with this prewarping technique only one frequency may be scaled properly and thus certain characteristics of continuous filters as roll-off per octave are not preserved. This method of synthesis is particularly well suited to synthesize low pass filters with a cut off frequency much smaller than the sampling frequency, because then the transformation function for the frequencies, $\omega = \frac{2}{T} \tan \frac{\Omega T}{2}$ may be considered linear, preserving then the characteristics of the continuous filter realization from which the

characteristics were obtained. This situation can be forced by increasing the sampling frequency or equivalently by decreasing the sampling interval T, and this solution could be the cure for all problems, but this is not so. As was discussed in chapter two, reducing the sampling interval, is equivalent to reducing the time available for computations, and for a fixed computing speed, this results in a reduction in the maximum complexity of the filters that can be implemented. Therefore, the reduction in the sampling interval is the least desirable tool to be used.

Besides this consideration of computing time, there is also another consideration about the number of bits required in the digital representation of the coefficients of the filter.

First it must be noted that the coefficients in the digital filters have a finite accuracy, and hence the location of the poles in the z plane is made on a discrete basis. To clarify this consider a simple example where the location of a pole is directly related to the coefficient accuracy. The filter

$$H(z) = \frac{1}{z - C_1} = \frac{z^{-1}}{1 - C_1 z^{-1}} \tag{3.35}$$

has a pole in the z plane located at the point $z = C_1$. Because of the finite accuracy in the representation of C_1 this pole can only be located at a finite number of positions. That is if a n bit binary representation of the coefficients is used, then the maximum accuracy in the pole position due to quantizing effect is 2^{-n}.

Consider then the effect of a reduction in the sampling interval on the mapping of the s plane into the z plane under the bilinear transformation.

To visualize this, a grid in the s plane, shown in Fig. 3.3, is mapped into the z plane using the bilinear transformation for values of T = 0.1, 0.05, 0.025, 0.125. The results are shown in Figs. 3.4, 3.5, 3.6 and 3.7.

As can be seen, the area in the z plane into which, a given area of the s plane is mapped decreases with T, the sampling interval. Conversely a given area in the z plane represents a larger area in the s plane as T decreases.

Consider a point z_1 in the z plane distant one quantizing level from the point z = 1 (towards the origin on the real axis) and distant one quantizing level along a vertical direction (above the real axis) as shown in Fig. 3.8.

$$z_1 = (1 - \xi_n) + j\,\xi_n \tag{3.36}$$

The corresponding point in the s plane is

$$s_1 = \frac{2}{T}\,\frac{z_1-1}{z_1+1} = \frac{2}{T}\,\frac{-\xi_n+j\,\xi_n}{2-\xi_n+j\,\xi_n} \tag{3.37}$$

$$= \frac{2}{T}\,\frac{\xi_n(-1+j1)(2-\xi_n-j\,\xi_n)}{(2-\xi_n)^2 + \xi_n^2} \tag{3.38}$$

$$= \frac{2}{T}\,\frac{\xi_n^2 - (2-\xi_n)\xi_n}{(2-\xi_n)^2 + \xi_n^2} + j\,\frac{(2-\xi_n - \xi_n)\,\xi_n}{(2-\xi_n)^2 + \xi_n^2} \tag{3.39}$$

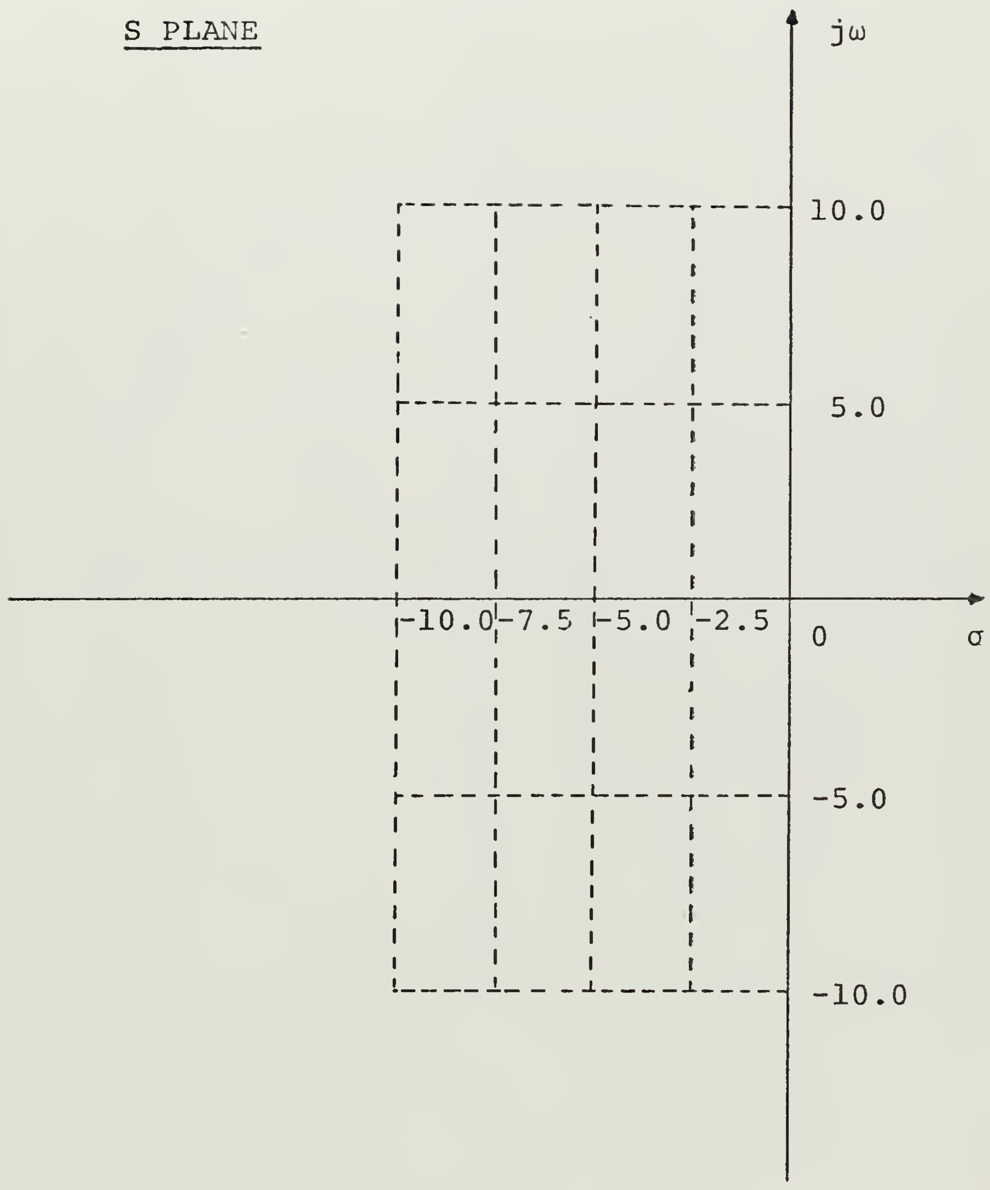

Fig. 3.3. Grid on the s plane to be mapped into the z plane using the bilinear transformation.

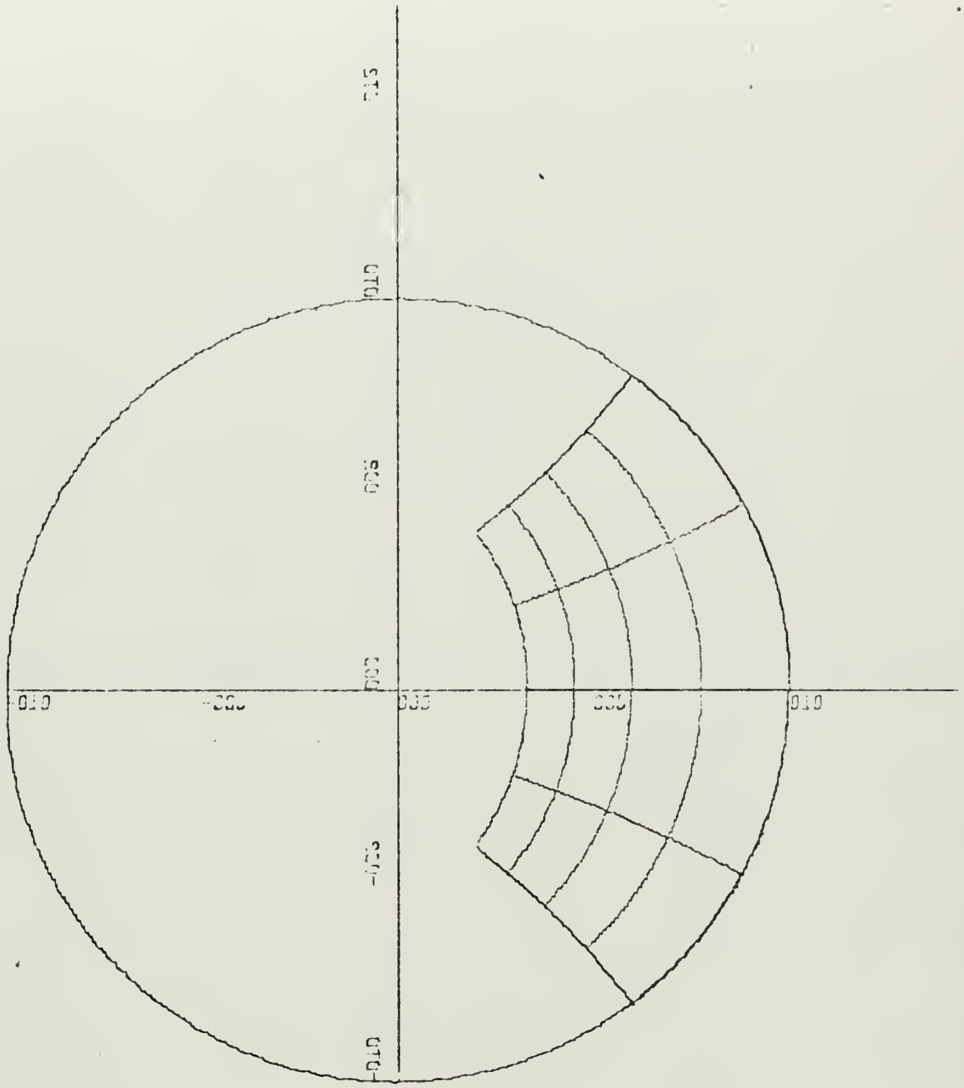

Fig. 3.4. Mapping of the grid of the s plane shown in Fig. 3.3, onto the z plane using the bilinear trnasformation for T = 0.1 sec.

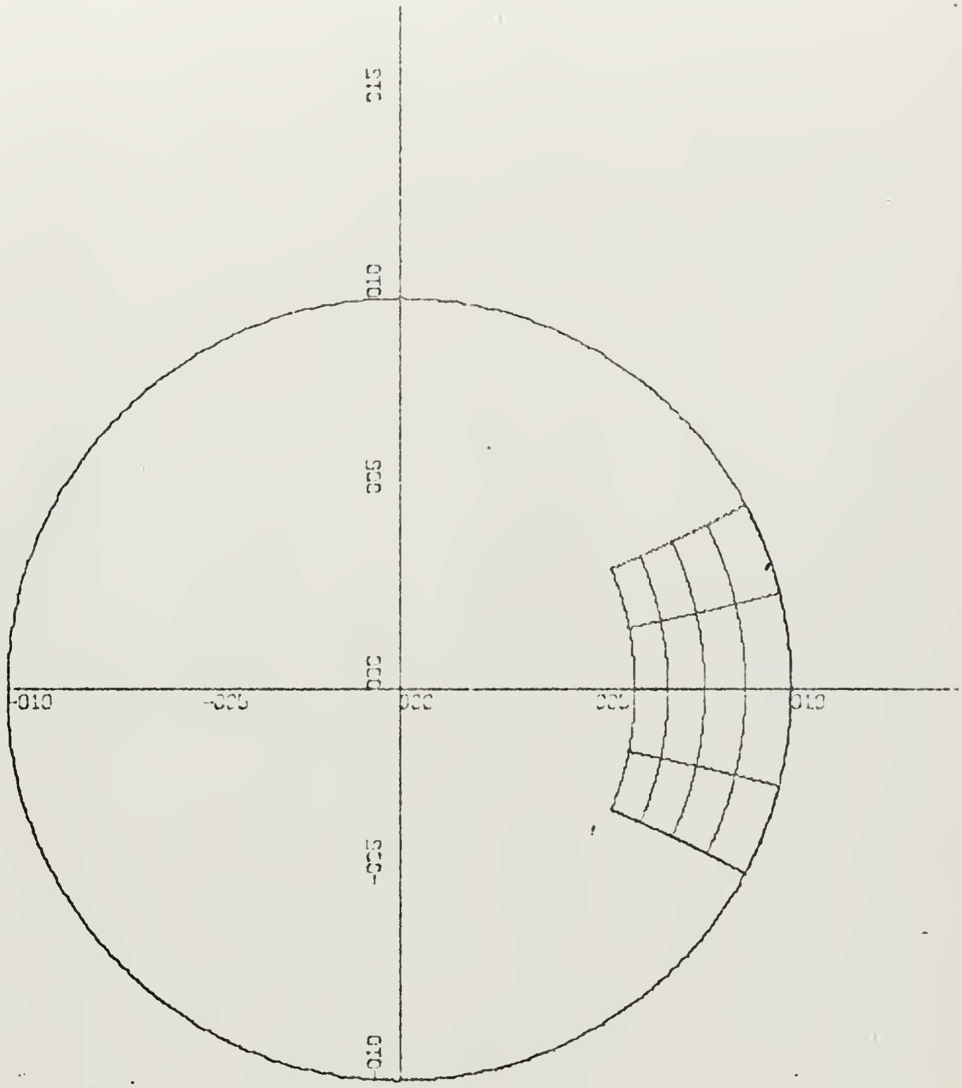

Fig. 3.5. Mapping of the grid of the s plane shown in Fig. 3.3 onto the z plane using the bilinear transformation for T = 0.05 sec.

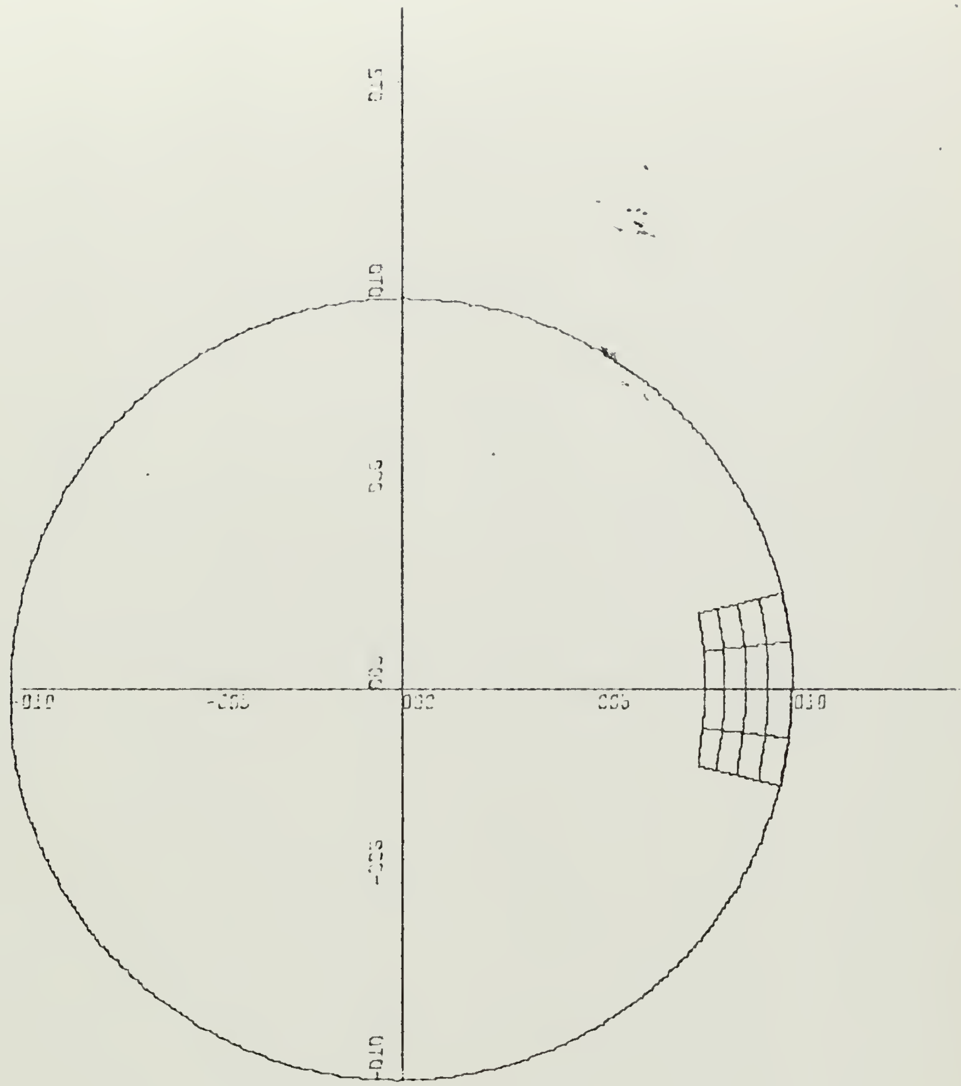

Fig. 3.6. Mapping of the grid of the s plane shown in Fig. 3.3 onto the z plane using the bilinear transformation for T = 0.025 sec.

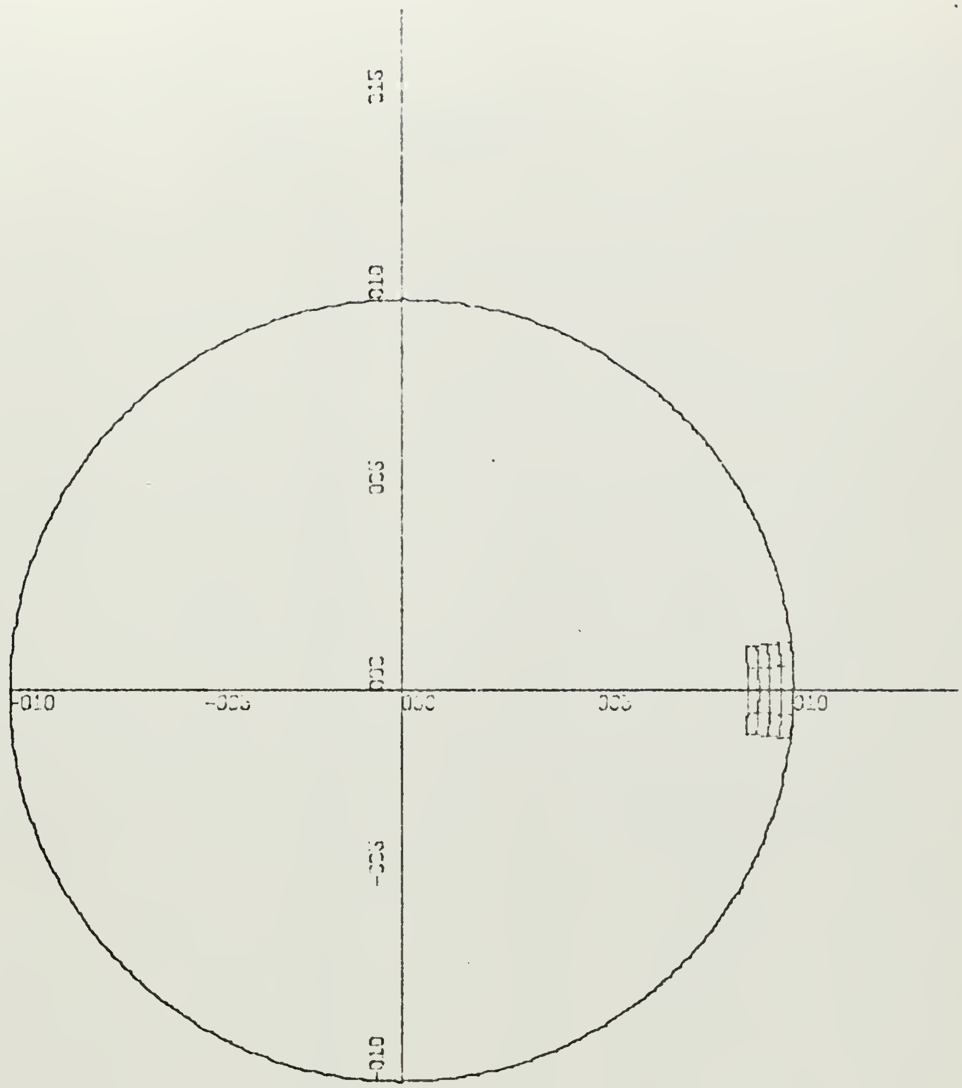

Fig. 3.7. Mapping of the grid of the s plane shown in Fig. 3.3 onton the z plane using the bilinear transformation for T = 0.0125 sec.

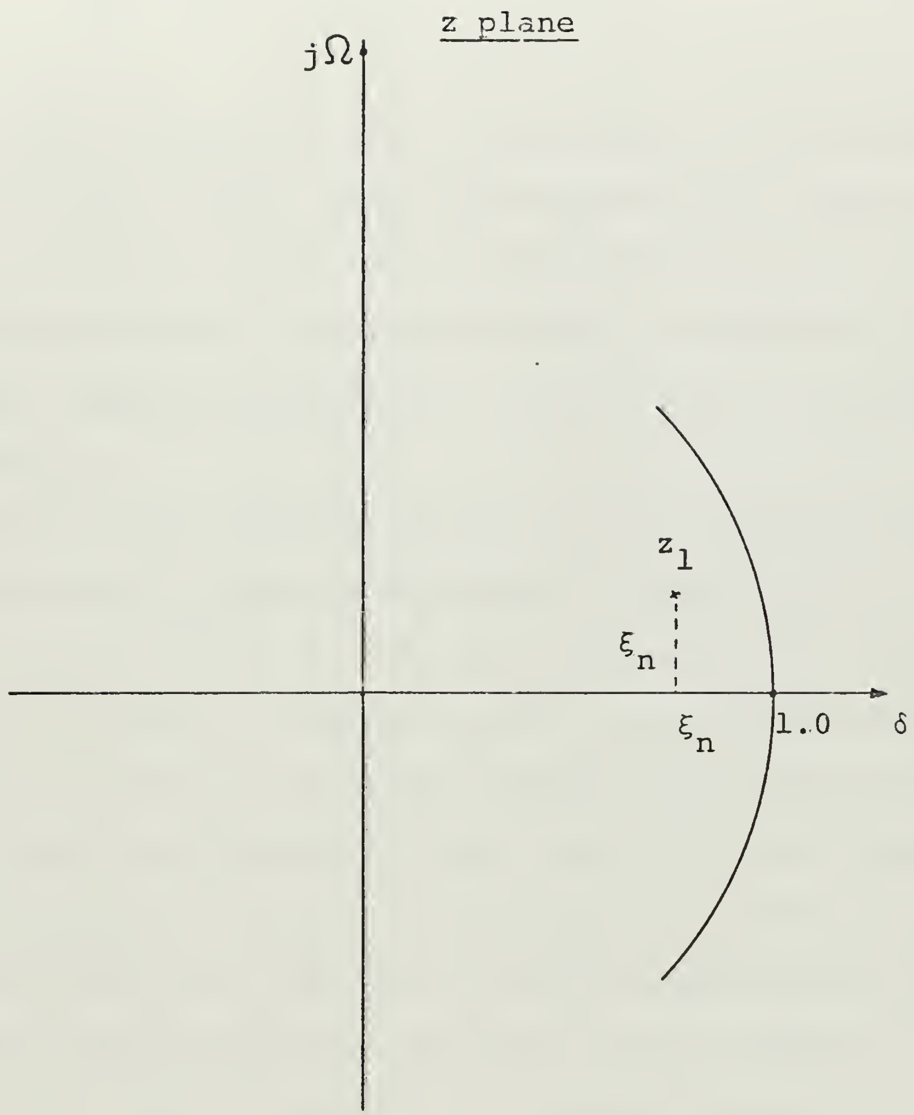

Fig. 3.8. Point $z = ((1-\xi_n), j\xi_n)$ distant one quantizing level from $z = 1.0$.

$$= \frac{2}{T} \quad \frac{\xi_n(\xi_n-1)2}{(2-\xi_n)^2 + \xi_n^2} + j \frac{\xi_n(1-\xi_n)2}{(2-\xi_n)^2 + \xi_n^2} \tag{3.40}$$

$$s_1 \simeq -\frac{\xi_n}{T} + j\frac{\xi_n}{T} \quad \text{where } \xi_n << 1 . \tag{3.41}$$

The above derivation can be considered as the mapping of a square of the z plane, each side measuring one quantizing level, ξ_n, into an area in the s plane of side ξ_n/T. Because of quantizing effects a singularity at z_i, can only be located at a finite number of positions, each of which corresponds to a position s_i.

Equation (3.41) indicates that the grainniness of allowed locations in the s plane is dependent on the quantizing level and the sampling interval. When using a continuous filter design to synthesize a digital filter, the pole locations so obtained may not be conincident with these allowed positions, and so it may be necessary to shift them to those allowed locations which are closest to the design locations. Due to other considerations, like pole location sensitivity in the s plane, the maximum shifting allowable in the location of a pole in the s plane may be limited to a maximum distance Δ. If it is desired to make the maximum allowable shifting comparable to the grainniness in the s plane the following equation may be established

$$\Delta = \frac{\xi_n}{T} \tag{3.42a}$$

In the z-plane this graininess would require n bits where

$$2^{-n} = \xi n \tag{3.42b}$$

From (3.42)

$$n = 3.3 \log \left(\frac{1}{\Delta T}\right) \tag{3.43}$$

where n represents the number of bits used in the binary representation of coefficients and Δ is an indication of the graininess of the grid in the s plane.

The lower bound of the required number of bits can be determined from Eq. (3.43). Actually, the required number may be more, especially if the poles are located very far from the origin in the s plane, because in this case the distortion in mapping of areas is bigger and can no longer be neglected in computing Δ through this derivation.

From the preceding discussion, it may be concluded that the finite representation of coefficients introduces an error in the location of the singularities of the function undergoing the transformation, and that this error increases, that is represents a larger change in the s plane when the sampling interval is decreased. In other words, it is not possible to obtain a better approximation by decreasing only the sampling interval. Instead the number of bits which represent the accuracy of the coefficients must simultaneously be increased to obtain a better approximation to the analog specification.

Because for real time operation all computations must be performed within a sampling interval, the above considerations

set a more rigorous limit than previously considered. This is so because an increase in bits to represent the coefficients tends to increase the computation time.

D. CONCLUSIONS

The algebraic substitution method provides an easy method to obtain a digital filter which approximates the characteristics of a continuous filter, providing then the desired link between the continuous filter theory and the discrete filter theory, with some restrictions.

Of all the substitutions, the bilinear transformation is the easiest to apply and does not increase the complexity of the filter, i.e., a n^{th} order continuous filter is transformed into a n^{th} order discrete filter.

The simulation of continuous systems obtained by the substitution technique in general can be improved by decreasing the sampling interval.

However, the spectrum obtained with a digital filter using this technique is only an approximation to the spectrum of the continuous filter from which it is derived, and if the continuous filter is itself an approximation to a given specification there is no assurance that the digital filter will also be within the specifications.

IV. SYNTHESIS OF DIGITAL FILTERS FROM FREQUENCY SPECTRUM CHARACTERISTICS

The standard Z transform technique and the algebraic substitution method considered in chapters two and three represent an attempt to extend the continuous filter theory to discrete or digital filter theory. There is no method available which will guarantee that a digital filter will have an exact replica of the frequency spectrum of the continuous filter from which it is derived, except when the input signal and the filter transfer function are band limited and sampled according to Shannon's theorem using the Z transform technique. When using the above methods to approximate the frequency characteristics of the continuous filters (which themselves are an approximation to certain given specifications) there is no assurance that the resulting digital filter will meet design specifications also.

A more direct approach to the study of the frequency spectra of digital filters seems to be necessary in order to provide better answers than the techniques derived from continuous filter theory.

A part of the material presented here is an extension of an idea mentioned by M. Martin [6], in which a nonrecursive filter is constructed. The approximation of Martin to a given specification using a Fourier series truncated at the n^{th} harmonic, requires 2 n words of storage and 2 n multiplications. The contribution described in this chapter leads to a recursive

filter, constructed from a ratio of two finite Fourier series approximating a given specification. This new procedure requires the same storage and number of multiplications, but allows one to obtain phase versus frequency characteristics other than the linear phase versus frequency with slope obtained when using Martin's method.

The last part of the chapter presents the development of a generalized technique to obtain recursive digital filters derived from a magnitude squared criterion. The magnitude squared function is expanded as a ratio of two finite Fourier series. For the approximating series to involve up to the n^{th} harmonic, this procedure requires only n words of storage, which represents a substantial improvement over the magnitude methods discussed in the early part of the chapter.

A. SYNTHESIS OF NONRECURSIVE FILTERS FROM A GIVEN MAGNITUDE SPECTRUM

In certain applications only the magnitude spectrum of the output signal is important and a time delay of some sampling intervals can be tolerated. The procedure that follows allows the given magnitude function to be approximated with a finite summation of terms of a Fourier series. This procedure is mentioned by M. Martin [6] with reference to data transmission filters.

Consider the elementary filter whose transfer function is of the form

$$H(z) = \frac{1}{2} [1+z^{-2}] \tag{4.1}$$

A flow diagram of the filter is shown in Fig. 4.1a.

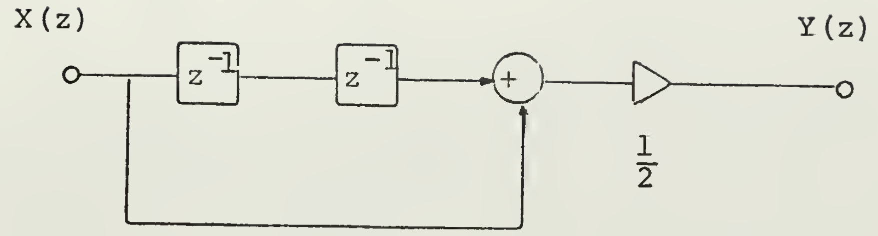

(a) The elementary filter of first order

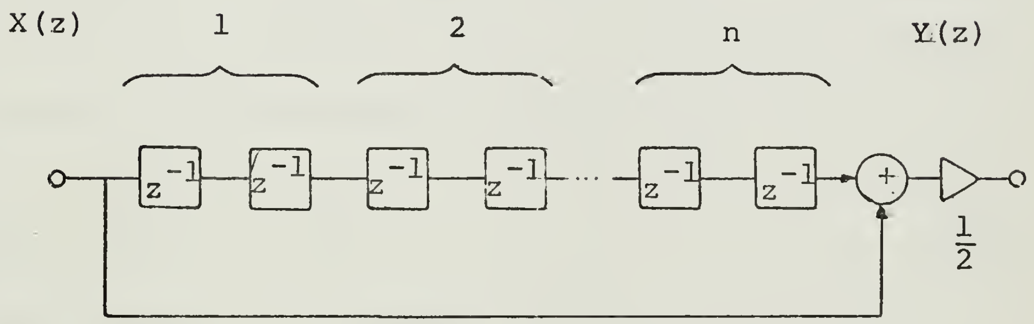

(b) The elementary filter of n^{th} order

Fig. 4.1. Elementary filters used for the Fourier series approximating technique

The elementary filter described has a spectrum of the form

$$H(e^{j\omega T}) = \frac{1}{2}[1 + e^{-j2\omega T}] \tag{4.2}$$

where $z = \exp(j\omega T)$ has been substituted in Eq. (4.1). Equation (4.2) can be reduced to the form

$$H(e^{j\omega T}) = \cos \omega T \; e^{-j\omega T} \tag{4.3}$$

and hence $$|H(e^{j\omega T})| = |\cos \omega T| \tag{4.4}$$

$$\text{Arg } H(e^{j\omega T}) = -\omega T \tag{4.5}$$

The elementary filter described in (4.1) is considered to be of order one and thus a family of elementary filters of higher order can be generated in the form of

$$H_n(z) = \frac{1}{2}[1 + z^{-2n}] \tag{4.6}$$

Such filters have frequency spectra of the form

$$H_n(e^{j\omega T}) = \cos n\omega T \; e^{-jn\omega T} \tag{4.7}$$

$$|H(e^{j\omega T})| = |\cos n\omega T| \tag{4.8}$$

$$\text{Arg } H(e^{j\omega T}) = -n\omega T \tag{4.9}$$

The filter of order n is illustrated in Fig. 4.1b.

Using these elementary filters it is possible to approximate any given magnitude versus frequency characteristic $|G(e^{j\omega T})|$, as will now be shown.

First it must be noted that if the output of any of these filters described in Eq. (4.6) is delayed m sampling intervals,

the frequency response becomes of the form

$$H_n(z) = \frac{1}{2}\,[1 + z^{-2n}] \cdot z^{-m} \tag{4.10}$$

$$H_n(e^{j\omega T}) = \cos n\omega T\; e^{-jn\omega T}\; e^{-jm\omega T}$$

$$= \cos n\omega T\; e^{-j(n+m)\omega T} \tag{4.11}$$

Comparing Eq. (4.11) with Eq. (4.7), it is clear that the magnitude of the frequency spectrum does not change by delaying the output. Only its phase changes in the form of an increase in the slope of the linear phase versus frequency characteristic.

Therefore, by delaying the output signal of these filters a convenient number of sampling intervals, it is possible to make their output signals have the same phase characteristics, and hence if several of these specially delayed filters are added in parallel, the resulting magnitude spectrum is the sum of the individual magnitude spectra because all the complex quantities to be added have the same phase.

An example of the above paragraph is illustrated in Fig. 4.2a where the elementary filters of zero and first order are delayed such that their phase versus frequency characteristic become equal to the second order elementary filter. In Fig. 4.2b the canonical form of the filter is shown, indicating symmetry in the coefficients.

Generalizing, a filter synthesized as a summation of the delayed elementary filters in the form

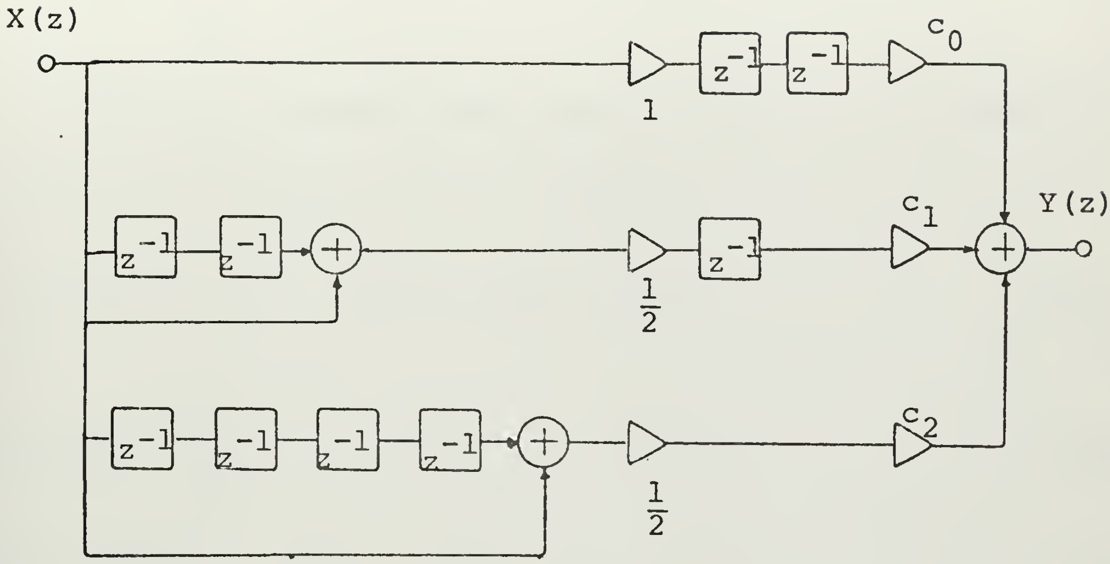

(a) Equation form

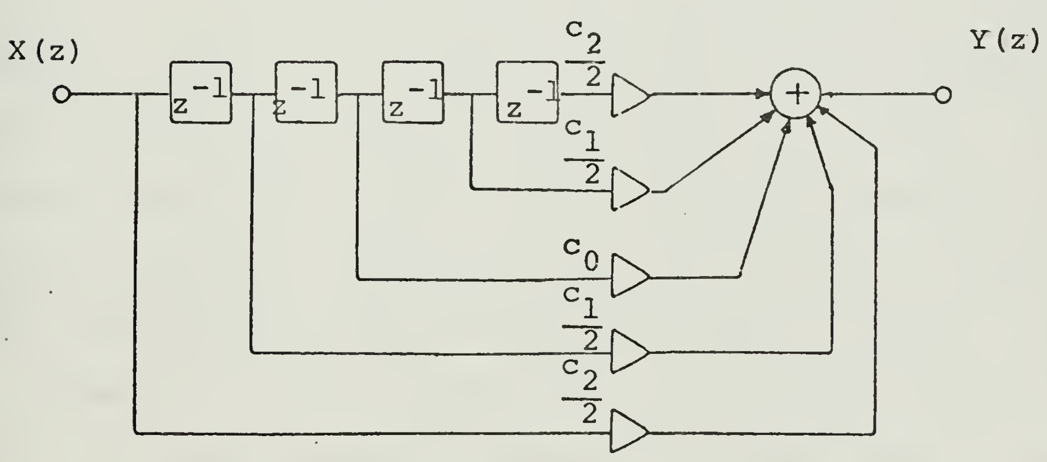

(b) Canonical form

$$\frac{Y(z)}{X(z)} = \frac{c_2}{2} + \frac{c_1}{2} z^{-1} + c_0 z^{-2} + \frac{c_1}{2} z^{-3} + \frac{c_2}{2} z^{-4}$$

Fig. 4.2. Synthesis of nonrecursive filter approximating a given spectrum function involving up to the second harmonic of the Fourier Series.

$$G(z) = \sum_{n=0}^{N} C_{\frac{n}{2}} [1 + z^{-2n}] \cdot z^{-N+n} \tag{4.12}$$

has a frequency spectrum which can be obtained by substituting = exp(jωT) into Eq. (4.12), yielding

$$G(e^{j\omega T}) = \sum_{n=0}^{N} C_n \cos n\omega T \ e^{-jN\omega T} \tag{4.13}$$

and hence $$|G(e^{j\omega T})| = |\sum_{n=0}^{N} C_n \cos n\omega T| \tag{4.14}$$

$$\operatorname{Arg} G(e^{j\omega T}) = - N\omega T \tag{4.15}$$

for real coefficients, C_n, with $(n=0,1,...,N)$.

Equation (4.14) indicates the possibility of approximating any given magnitude spectrum with a Fourier series of finite numbers of terms. It is known that the magnitude spectra are even functions, and repetitive with period $\omega_s = 2\pi/T$. This characteristic assures that it will always be possible to expand a magnitude spectrum function as a Fourier series with cosine terms only, assuring also the generality of Eq. (4.14).

Equation (4.15) indicates that the resulting function will be delayed N sampling intervals, N being equal to the number of harmonics considered in the Fourier series expansion.

$$\text{If } \sum_{n=0}^{N} C_n \cos n\omega T \geq 0 \quad \text{for all } \omega \tag{4.16}$$

then the phase given by Eq. (4.15) will not display any discontinuity jumps and will remain linear. This can always be accomplished by proper adjustement of the coefficient C_0.

It is well known that the Gibb's phenomenon occurs near a discontinuity of a function. In other words no matter how many harmonics are considered in the Fourier series approximation, the summation of terms does not converge to the value of the function near a discontinuity, but does converge to an overshoot and a undershoot of approximately 10% of the discontinuous jump. In order to make certain that (4.16) is satisfied, the value of C_0 must be adjusted to include the undershoot of the Gibb's phenomenon. In the case of an ideal low pass filter the Gibb's phenomenon is about 10% of the discontinuity. If C_0 is adjusted so that the Fourier series is always positive, this implies that the attenuation in the stop band is approximately 20 db.

Some other methods may be used to obtain a greater attenuation. For instance the Lanczos and Fejer methods to attenuate or eliminate the overshoot and ripple of the Fourier series can be used as discussed by R. W. Hamming [12].

A different approach to get around this inconvenience is to work numerically, with the given magnitude spectrum as a set of data points, through which a continuous function is to be fitted. The lack of discontinuities assures that Gibb's phenomenon will not occur.

A simple example of nonrecursive digital filter synthesis is now presented.

Synthesize a nonrecursive digital low pass filter approximating the magnitude function shown in Fig. 4.3, where $\omega_c = \pi/3T$ and the order of the filter is chosen such that the approximation involves the fourth harmonic in the Fourier series expansion.

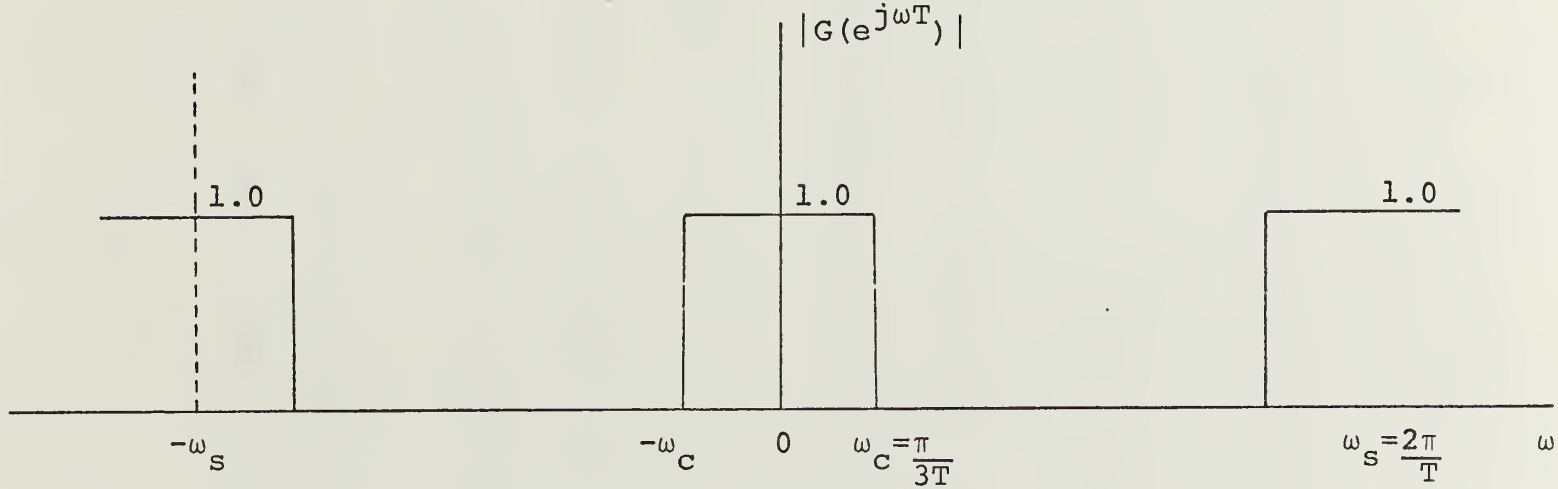

Fig. 4.3. Magnitude versus frequency characteristic to be matched with a digital filter.

Representing the magnitude function as a Fourier series yields

$$|G(e^{j\omega T})| = \frac{C_o}{2} + \sum_{n=1}^{4} C_n \cos n\omega T$$

where $C_n = \dfrac{4}{\omega_s} \displaystyle\int_o^{\omega_c} \cos n\omega T \, d\omega = \dfrac{4}{\omega_s} \dfrac{1}{nT} \sin n\omega T \Big|_o^{\omega_c}$

$$= \frac{4}{nT\omega_s} \sin nT\omega_c \qquad = \frac{4\omega_c}{\omega_s} \cdot \frac{\sin nT\omega_c}{nT\omega_c}$$

For this example $\omega_c/\omega_s = 1/6$ and $\omega_c T = \pi/3$.

Therefore the coefficients C_n become

$$C_n = \frac{2}{3} \; \frac{\sin n \; \pi/3}{n \; \pi/3}$$

$C_0 = 0.66666 \quad C_1 = 0.55133 \quad C_2 = 0.27567 \quad C_3 = 0.00 \quad C_4 = -0.13783$

Consider first the case where C is not adjusted so that (4.16) is not satisfied.

$$|G(e^{j\omega T})| = 0.33333 + 0.55133 \cos \omega T + 0.27567 \cos 2\omega T$$

$$+ 0.0 \cos 3\omega T - 0.13783 \cos 4\omega T$$

and from Eqs. (4.14) and (4.12)

$$G(z) = 0.33333 \, z^{-4} + \frac{0.55133}{2} [1 + z^{-2}]z^{-3} + \frac{0.27567}{2}$$

$$[1 + z^{-4}]z^{-2} - \frac{0.13783}{2} [1 + z^{-2}]$$

and rearranging terms the filter becomes

$$G(z) = -0.068915 + 0.13783\, z^{-2} + 0.27567\, z^{-3} + 0.33333\, z^{-4} + 0.27567\, z^{-5} + 0.13783\, z^{-6} - 0.068915\, z^{-8}$$

In Figs. 4.4 and 4.5 the magnitude and phase versus frequency characteristics are shown for the filter of the example, where the coefficients are obtained directly from the Fourier series expansion. The discontinuities in the phase function can be seen to correspond to every cross over point shown in the magnitude function by an increase in attenuation. The lobes in the attenuation band of the magnitude function are the ripples of the Fourier series but distorted by the logarithmic scale. If C_0 is adjusted so that $C_0 = 0.46030$ then

$$G(z) = -0.068915 + 0.13783\, z^{-2} + 0.27567\, z^{-3} + 0.46030\, z^{-4} + 0.27567\, z^{-5} + 0.13783\, z^{-6} - 0.068915\, z^{-8}$$

The magnitude and phase response of this filter are shown in Figs. 4.6 and 4.7.

In general the foregoing procedure requires 2 n words of storage for n harmonics considered in the Fourier series approximation. Furthermore the output signal has a delay of n sampling intervals due to the remarkable characteristic of this type of filters of having a linear phase with a slope dependent only in the number of delays of the filter, Failure to observe the condition stated in Eq. (4.16) produces discontinuities in the phase characteristic associated with each crossing of the ω axis by the resulting Fourier series.

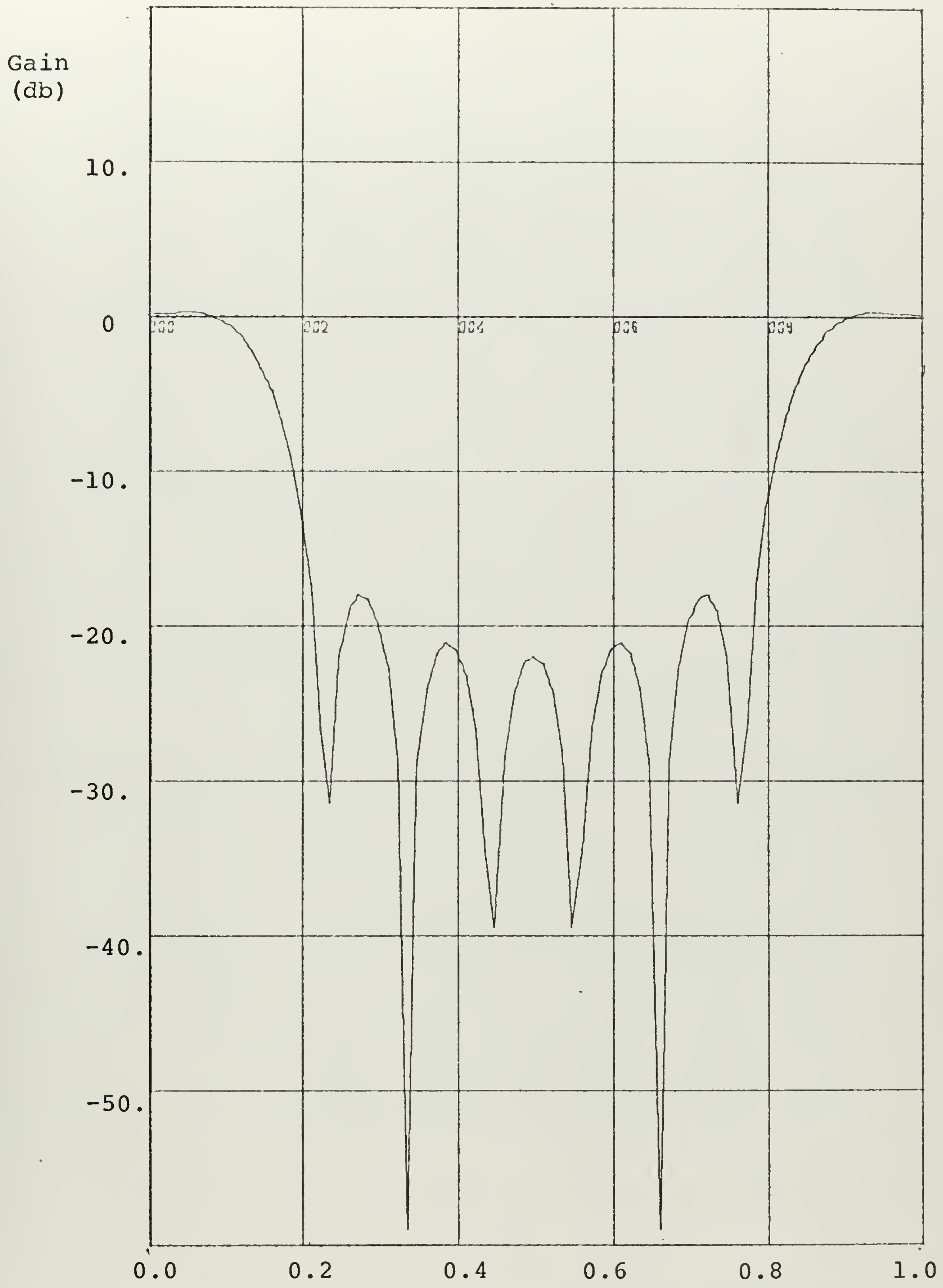

Fig. 4.4 Magnitude vs. normalized frequency. Non-recursive filter with coefficients from Fourier series.

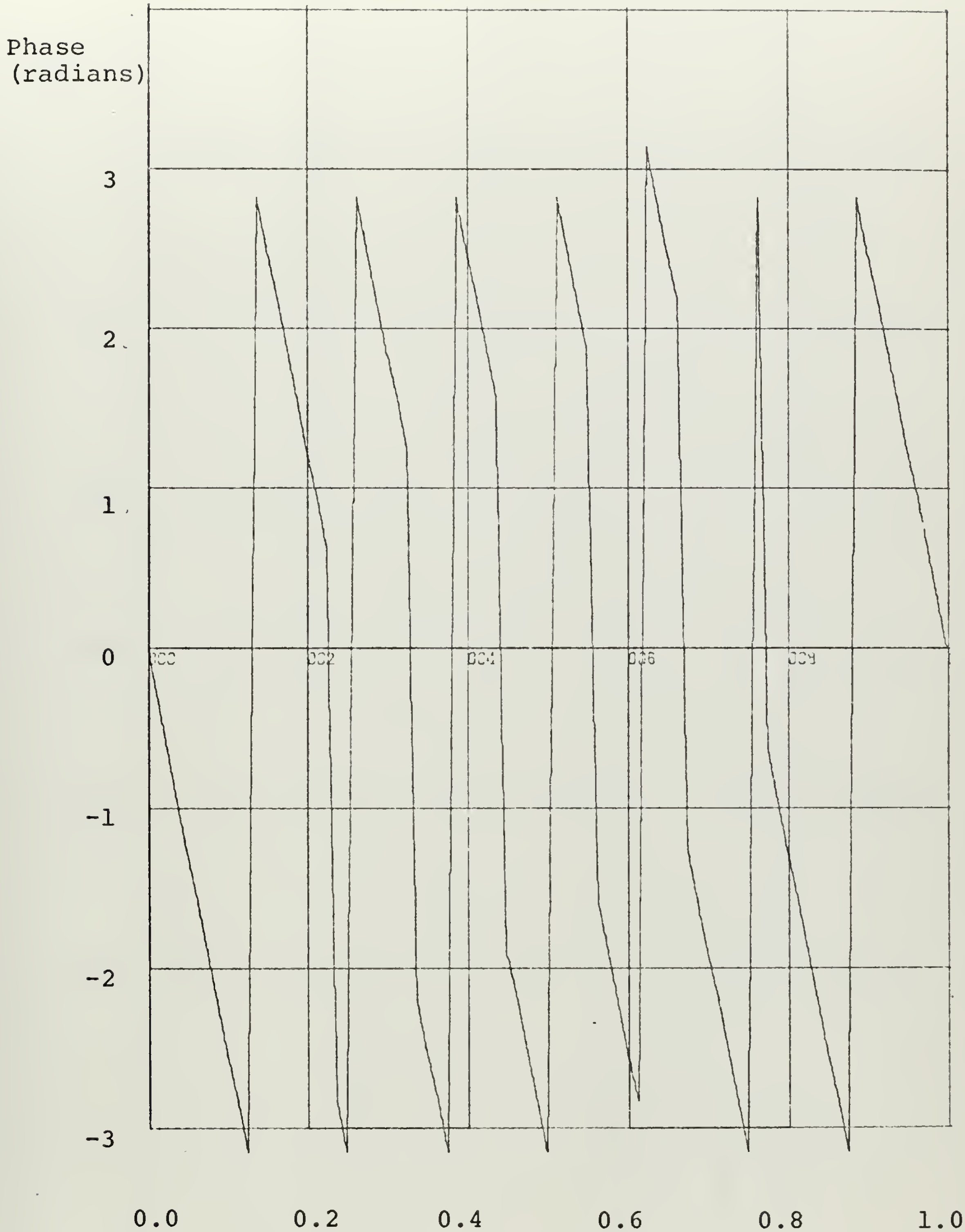

Fig. 4.5 Phase vs. normalized frequency. Non-recursive filter with coefficients obtained from Fourier series.

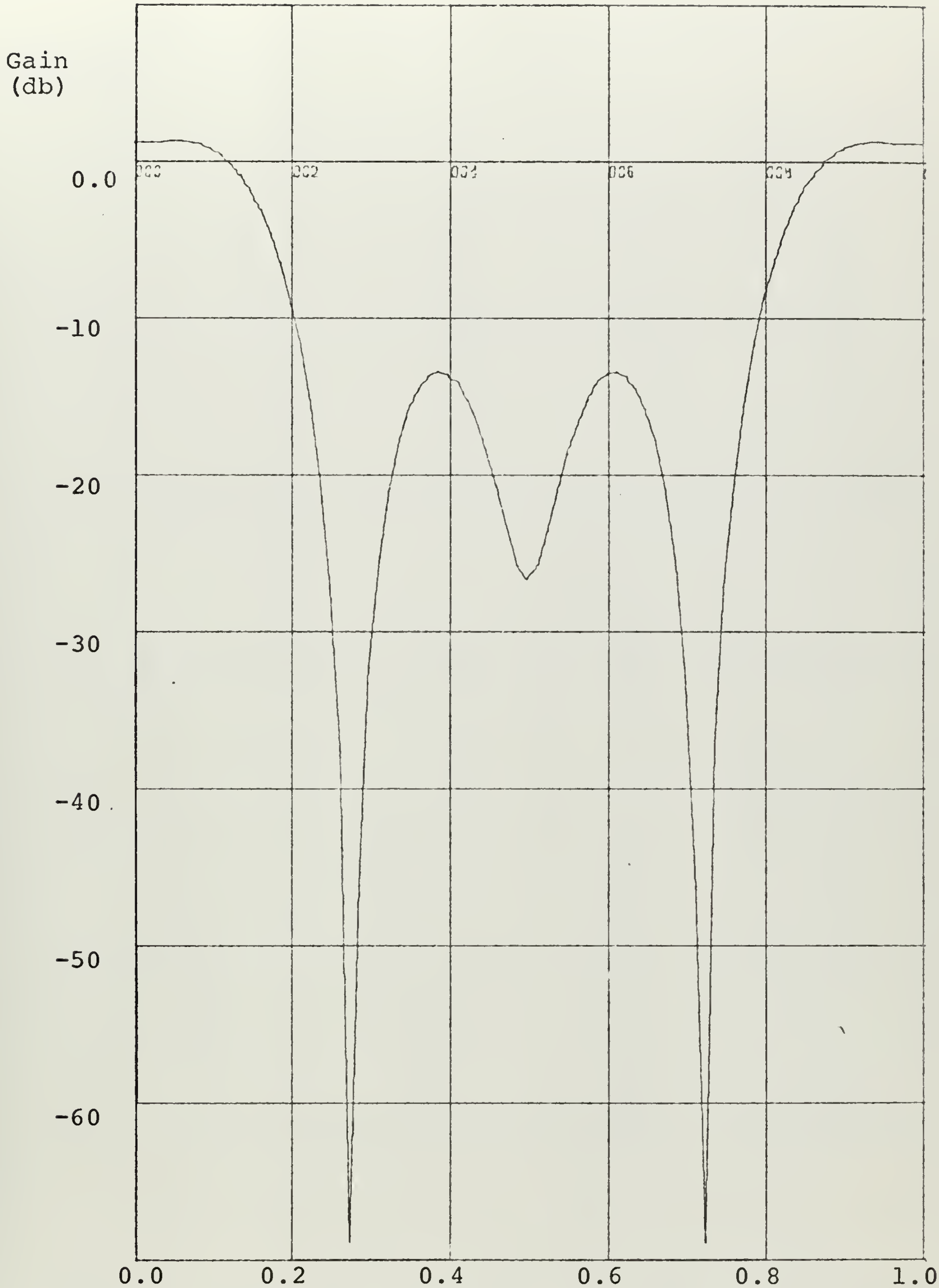

Fig. 4.6 Magnitude vs. normalized frequency. Non-recursive filter, coefficients obtained from modified Fourier series to obtain linear phase.

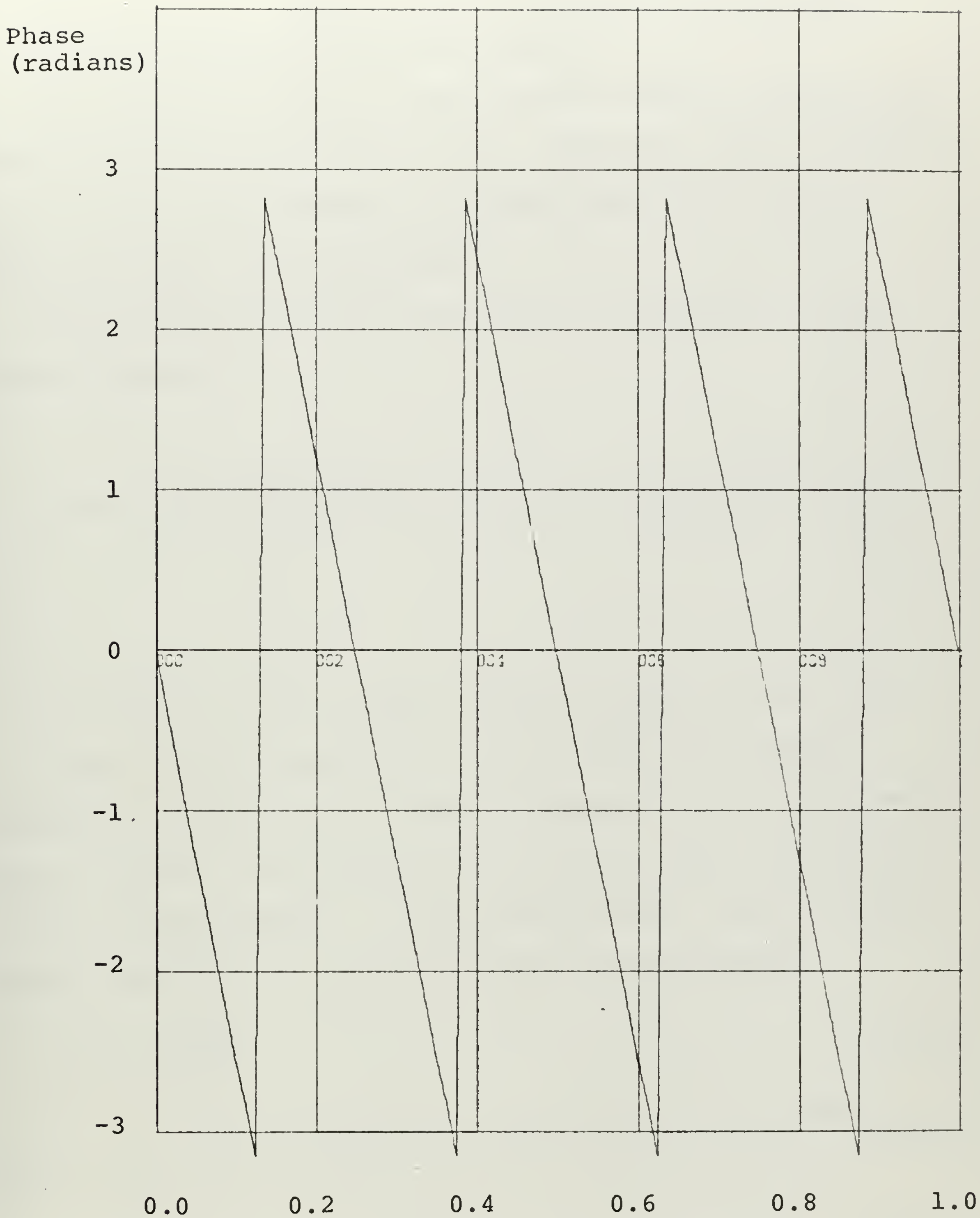

Fig. 4.7 Phase vs. normalized frequency. Nonrecursive filter, coefficients obtained from modified Fourier series to obtain linear phase.

B. SYNTHESIS OF A SPECIAL TYPE OF RECURSIVE FILTER FROM A GIVEN MAGNITUDE SPECTRUM FUNCTION

The method described in the previous section, where non-recursive filters were obtained for matching a given magnitude function, has been generalized by the author and allows a recursive filter to be obtained.

This special type of filter has a Z transform of the impulse response

$$H(z) \quad \frac{a_n + a_{n-1}z^{-1} + \ldots + a_0 z^{-n} + \ldots + a_{n-1}z^{-2n+1} + a_n z^{-2n}}{b_m + b_{m-1}z^{-1} + \ldots + b_o z^{-m} + \ldots + b_{m-1}z^{-2m+1} + b_m z^{-2m}} \tag{4.17}$$

A canonical form of this filter is shown in Fig. 4.8.

Note that the polynomials of the numerator and the denominator have an even number of delays for the input and output signals, and furthermore are mirror image polynomials because of the symmetry in the coefficients. Such a filter can be considered to be derived from the expression

$$H(z) = \frac{A(z)}{B(z)} \tag{4.18}$$

where $$A(z) = \overline{a_n + a_{n-1}z^{-1} + \ldots + a_0 z^{-n} + \ldots + a_{n-1}z^{-2n+1} + a_n z^{-2n}} \tag{4.19}$$

and $$B(z) = \overline{b_m + b_{m-1}z^{-1} + \ldots + b_0 z^{-m} + \ldots + b_{m-1}z^{-2m+1} + b_m z^{-2m}} \tag{4.20}$$

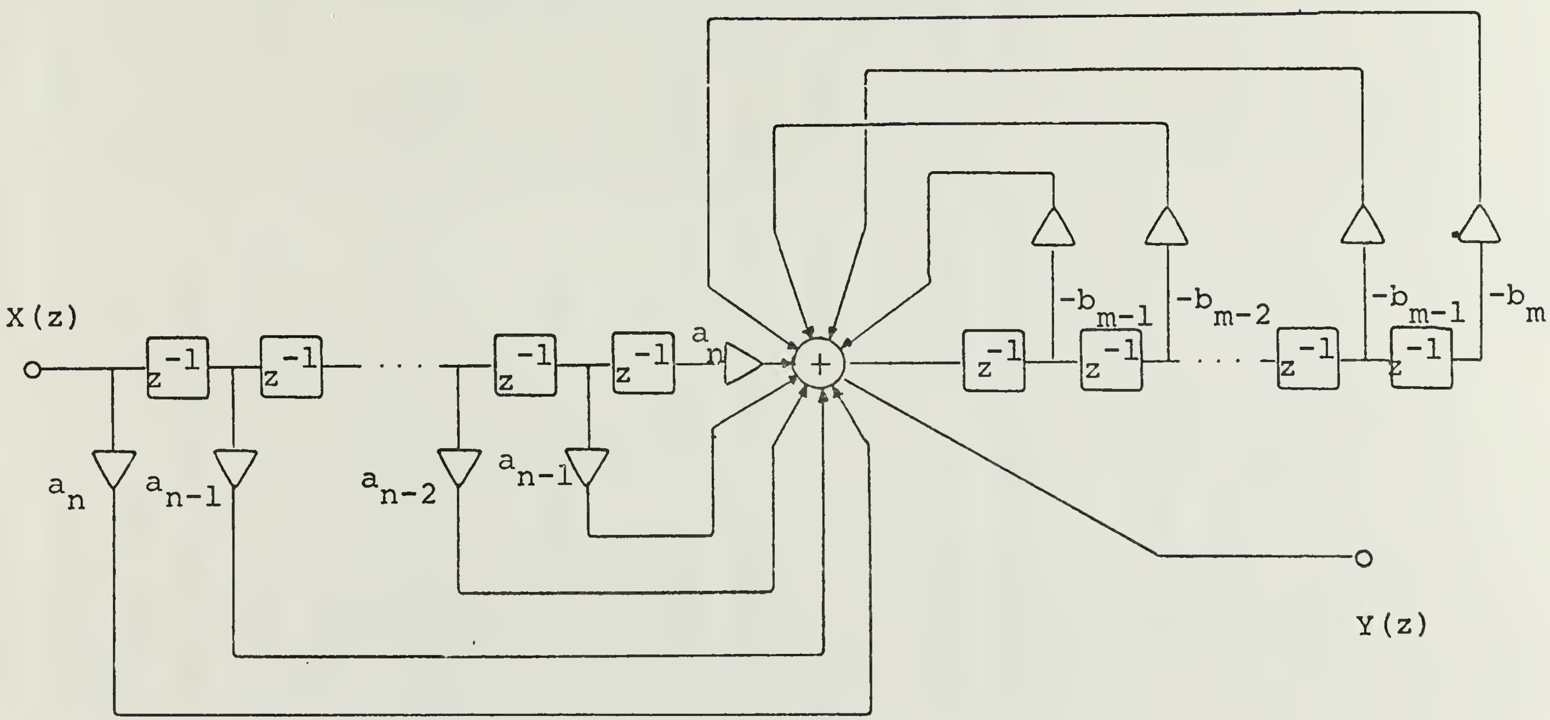

Fig. 4.8. Special type filter with 2 n delays for input and output signals and symetric coefficients.

The frequency spectrum of such a filter is given by

$$H(e^{j\omega T}) = \frac{A(e^{j\omega T})}{B(e^{j\omega T})} \qquad (4.21)$$

and from Eqs. (4.12)and (4.13)

$$H(e^{j\omega T}) = \frac{a_o + \sum_{k=1}^{n} 2a_k \cos k\omega T}{b_o + \sum_{k=1}^{m} 2b_k \cos k\omega T} e^{-j(n-m)\omega T} \qquad (4.22)$$

Equation (4.22) shows the properties of this special type of filter being considered. It indicates that its frequency spectrum is in the form of a ratio of two finite Fourier series, and the phase is linear with respect to frequency.

When a magnitude versus frequency characteristic is given to be approximated with a digital filter, if an approximation in the form of the ratio of two finite Fourier series can be obtained, then a method to synthesize the filter is available by using Eq. (4.22) as will now be explained.

1. The Expansion of a Magnitude Function as a Ratio of Two Finite Fourier Series

Consider first the properties of the Chebyshev polynomials, as discussed for instance by R. W. Hamming [13].

"The Chebyshev polynomials have all the properties of both the Fourier series and the orthogonal polynomials; they are, in fact, the Fourier functions cos n θ in the disguise of a simple transformation of the variable

$\theta = \arccos x$ "

If a variable x is defined such that

$$x = \cos \omega T \tag{4.23}$$

from where $-1 \leq X \leq 1$

then,

$$T_n(x) = \cos (n \text{ arc} \cos x) = \cos (\omega T \eta) \tag{4.24}$$

In view of Eq. (4.24) an expansion in Chebyshev polynomials in the variable x corresponds to a Fourier series in the variable ωT, when the two variables are related as in Eq. (4.23). This property can be used to approximate a given magnitude spectrum function as a ratio of two finite Fourier series in the following manner:

Given a function $|G(e^{j\omega T})|$ which has to be approximated consider the following transformation

$$|G(e^{j\omega T})| = G_1(\omega T) = G_1(\text{arc} \cos x) = H(x) \tag{4.25}$$

If this is done numerically, that is if pairs of values describing points of the magnitude versus frequency characteristic are given Eq. (4.25) can be considered as a change in the ωT values of the given points, maintaining the ordinate values. The interest in doing this is that now the new function of x can be approximated as a ratio of two polynomials in x. Later the polynomials may be expressed as Chebyshev polynomials and then use of the property described in (4.24) leads to the Fourier series coefficients. That is

H(x) can be approximated by

$$H(x) \approx \frac{P_n(x)}{Q_m(x)} \tag{4.26}$$

and numerator and denominator polynomials can be represented as an expansion of Chebyshev polynomials of the form

$$H(x) \approx \frac{\sum_{k=0}^{n} c_k \, T_k(x)}{\sum_{k=0}^{m} d_k \, T_k(x)} \tag{4.27}$$

Using the property of Eq. (4.24)

$$|G(e^{j\omega T})| \approx \frac{\sum_{k=0}^{n} c_k \cos k\omega T}{\sum_{k=0}^{m} d_k \cos k\omega T} \tag{4.28}$$

and Eq. (4.28) represents the approximation of a given function as the ratio of two finite Fourier series.

For synthesis purposes, the coefficients in Eq. (4.28) can be equated with those of Eq. (4.22) yielding

$$a_k = c_k \qquad k \neq 0 \tag{4.29}$$

$$b_k = d_k \qquad k \neq 0 \tag{4.30}$$

The complete synthesis procedure is illustrated in Fig. 4.9. The following points should be noted:

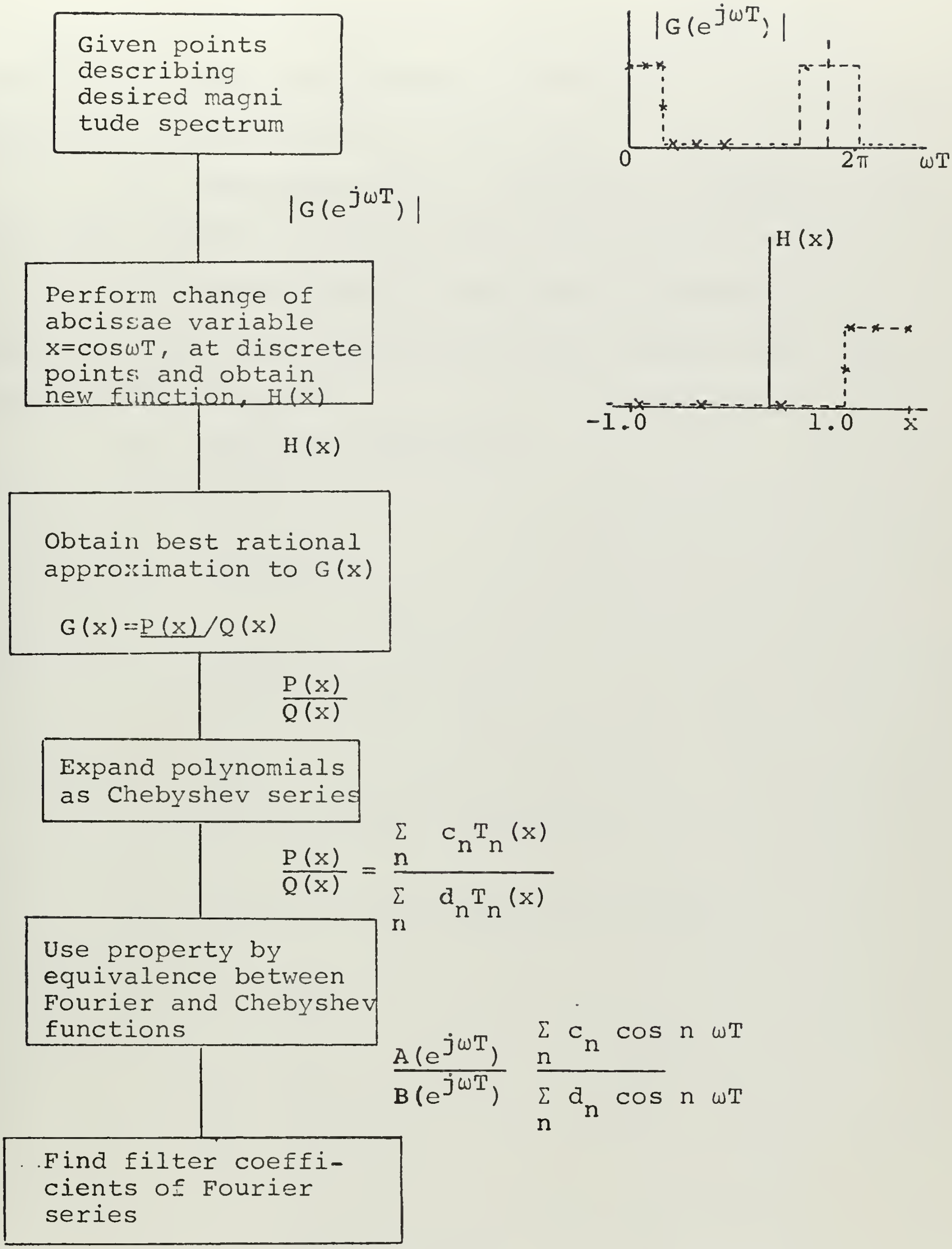

Fig. 4.9. Procedure to find an approximating function to a given set of data points, in the form of the ratio of two finite Fourier series with cosine terms only.

a. If the discrete steps in the abcissae of $|G(e^{j\omega T})|$ are uniformly spaced, the abcissae of $H(x)$ will be nonuniformly spaced since $x_k = \cos \omega_k T$.

b. Expressing $H(x) = P(x)/Q(x)$ is possible in many ways. For the work presented here IBM subroutine ARAT is used.

c. Expressing $P(x)$ and $Q(x)$ as Chebyshev polynomials is performed using the following tables taken from McCracken and Dorn [14].

1. Chebyshev Polynomials

$$T_0(x) = 1$$

$$T_1(x) = x$$

$$T_2(x) = 2\,x^2 - 1$$

$$T_3(x) = 4\,x^3 - 3\,x$$

$$T_4(x) = 8\,x^4 - 8\,x^2 + 1$$

$$T_5(x) = 16\,x^5 - 20\,x^3 + 5\,x$$

2. Powers of x as functions of $T_n(x)$

$$1 = T_0$$

$$x = T_1$$

$$x^2 = \tfrac{1}{2}(T_0+T_2)$$

$$x^3 = \tfrac{1}{4}(3T_1+T_3)$$

$$x^4 = \tfrac{1}{8}(3T_0+4T_2+T_4)$$

$$x^5 = \tfrac{1}{16}(10T_1+5T_3+T_5)$$

The degree of the numerator and denominator polynomials can be different, as indicated in Eq. (4.30). The

difference in polynomial degree has direct influence on the phase characteristics, as shown in Eq. (4.22). Selecting equal degrees for numerator and denominator, it is possible to make the phase equal to zero for all frequencies. Otherwise the phase will change linearly with frequency, and the slope will be directly proportional to the difference in degree.

An example of synthesis using this procedure is now presented. For comparison with the M. Martin method, the example given in the previous section is reworked. The magnitude spectrum of Fig. 4.3 will be approximated using a filter with eight delays, four in the numerator and four in the denominator, which implies the approximation of the given magnitude spectrum with a ratio of two Fourier series involving up to the second harmonic in each. The method used in the example to obtain the ratio of two Fourier series approximating the given magnitude spectrum function, is the numerical method illustrated in Fig. 4.9, using subroutine ARAT of the IBM scientific package to obtain the ratio of two polynomials in the transformed variable $x = \cos \omega T$. The results are:

Given eight points describing the magnitude spectrum function equally spaced on the ωT axis in the range

$$0 \leq \omega T \leq \pi \tag{4.31}$$

The change to the variable x is performed and a ratio of two polynomials in x approximating the points was found

$$H(x) = \frac{0.01184 + 0.02418\ x + 0.01277\ x^2}{1.000 - 1.39494\ x + 0.47740\ x^2} \tag{4.32}$$

The polynomials are now expanded in terms of Chebyshev polynomials using table shown previously. This yields

$$H(x) = \frac{0.01823\ T_0(x) + 0.02418\ T_1(x) + 0.00639\ T_2(x)}{1.23870\ T_0(x) - 1.39494\ T_1(x) + 0.23870\ T_2(x)} \quad (4.33)$$

Using Eq. (4.24) the ratio of Fourier series can be obtained.

$$|G(e^{j\omega T})| = \frac{0.01823 + 0.02418 \cos \omega T + 0.00639 \cos 2\omega T}{1.23870 - 1.39494 \cos \omega T + 0.23870 \cos 2\omega T} \quad (4.34)$$

From Eqs. (4.22) and (4.28) it follows that

$$G(z) = \frac{0.00319+0.01209z^{-1}+0.01823z^{-2}+0.01209z^{-3}+0.00319z^{-4}}{0.11935-0.69747z^{-1}+1.23870z^{-2}-0.69747z^{-3}+0.11935z^{-4}} \quad (4.35)$$

The magnitude and phase of the spectrum has been plotted and illustrated in Figs. 4.10a and 4.10b. As a comparison with M. Martin's method shown in Fig. 4.4, it can be noted that there is an increase in attenuation and elimination of lobes as well as zero phase shift.

C. SYNTHESIS OF RECURVSIVE FILTERS FROM MAGNTIDUE SQUARED FREQUENCY SPECTRUM FUNCTIONS

In the previous section the filter is restricted to a minor image coefficient realization starting with the magnitude of a transfer function. In this section a new approach is developed to synthesize recursive digital filters, from a given magnitude squared function.

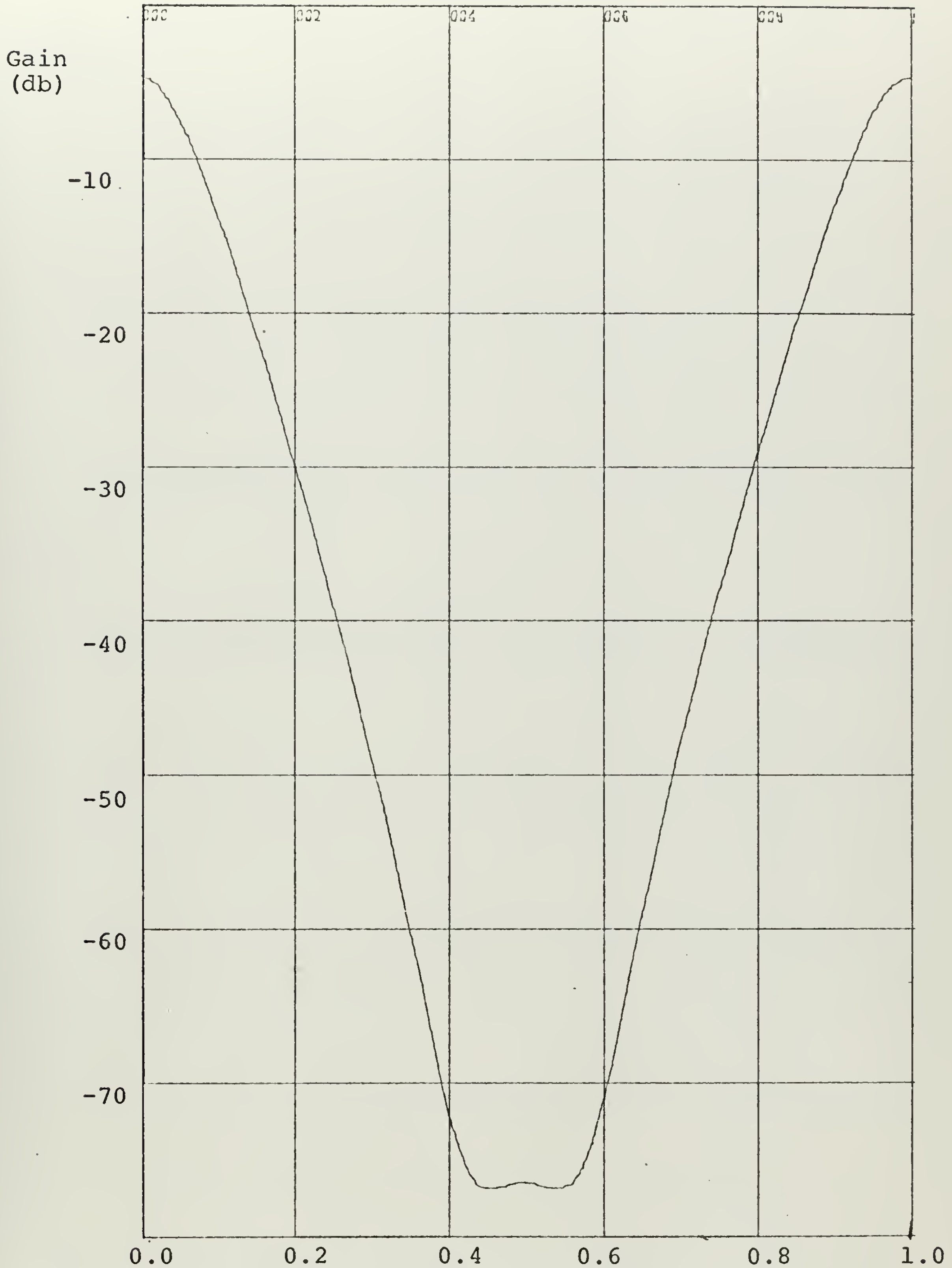

Fig. 4.10a Magnitude vs. normalized frequency. Recursive filter, coefficients obtained from numerical approximation described in Fig. 4.8.

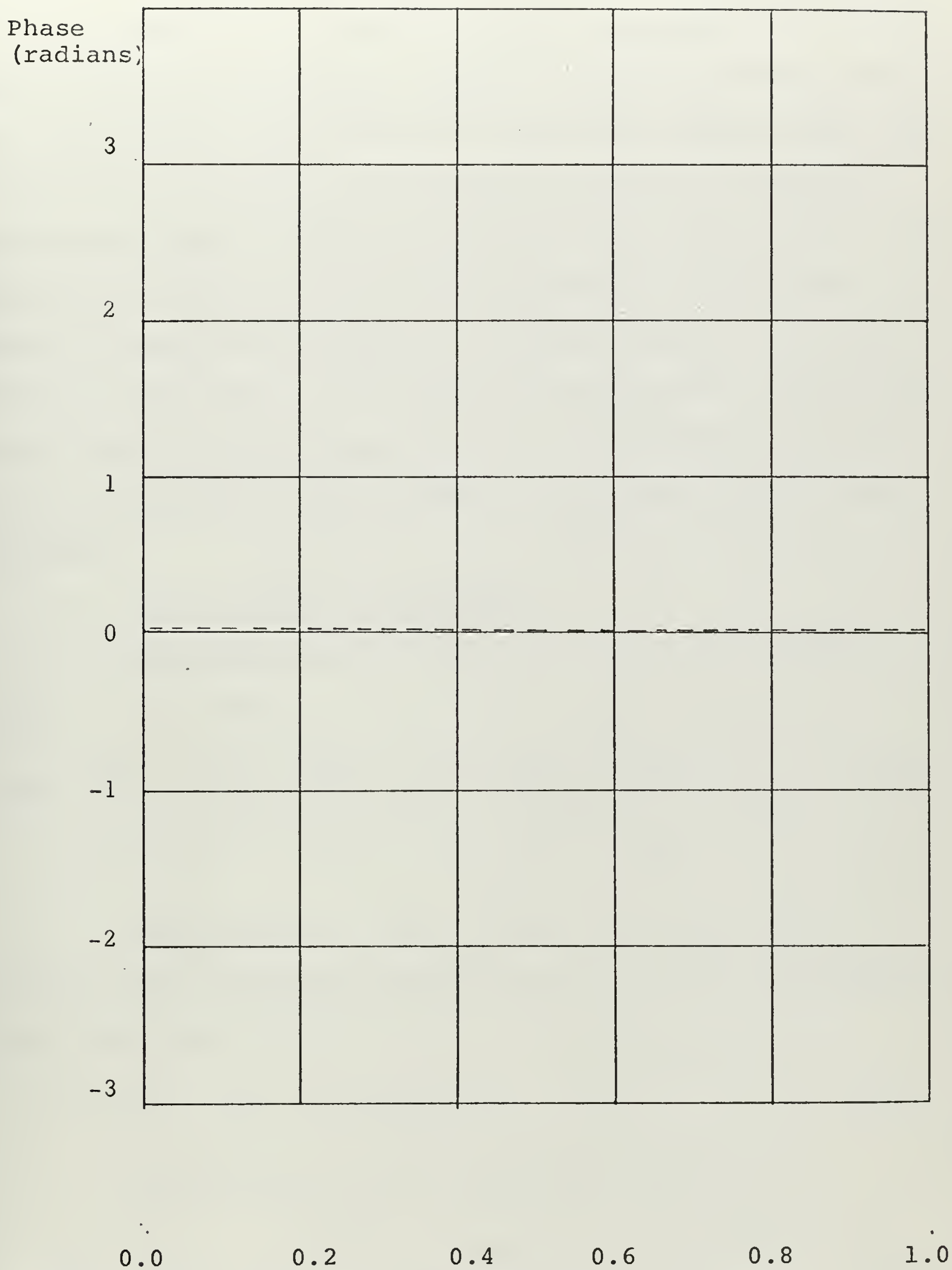

Fig. 4.10b Phase vs. normalized frequency. Recursive filter, coefficients obtained from numerical approximation described in Fig. 4.8.

It is shown that a digital filter, described in its most general form has a magnitude squared frequency spectrum which is a ratio of two finite Fourier series with cosine terms only. A method for obtaining an approximation to such a function, has been described in the previous section, using a change of variable and expansion of the approximating function in a series of Chebyshev polynomials. In this section the coefficients of the filter are obtained by equating the coefficients of the Fourier series expansion with the coefficients of the filter according to some nonlinear relationships which are developed.

1. Developement of the Theory

Consider a generalized description of a digital filter, of the form

$$H(z) = \frac{a_0 + a_1 z^{-1} + a_2 z^{-2} + \ldots + a_k z^{-k}}{b_0 + b_1 z^{-1} + b_2 z^{-2} + \ldots + b_m z^{-m}} = \frac{\sum_{j=0}^{k} a_j z^{-j}}{\sum_{i=0}^{m} b_k z^{-i}} \tag{4.36}$$

The spectrum of this filter can be obtained by evaluating the magnitude and phase of Eq. (4.17) for values of z along the unit circle

$$z = e^{j\omega T} = \cos \omega T + j \sin \omega T \tag{4.37}$$

Substituting (4.37) into (4.36), yields

$$H(e^{j\omega T}) = \frac{a_0 + a_1 e^{-j\omega T} + a_2 e^{-j\omega T} + \ldots + a_k e^{-jk\omega T}}{b_0 + b_1 e^{-j\omega T} + b_2 e^{-j\omega T} + \ldots + b_m e^{-jm\omega T}} \tag{4.38}$$

Consider

$$H(e^{j\omega T}) = \frac{N(j\omega)}{D(j\omega)}$$

$$|H(e^{j\omega T})|^2 = \frac{|N(j\omega)|^2}{|D(j\omega)|^2}$$

$$|H(e^{j\omega T})|^2 = \frac{Re^2\{N(j\omega)\} + Im^2\{N(j\omega)\}}{Re^2\{D(j\omega)\} + Im^2\{D(j\omega)\}} \tag{4.39}$$

$$|H(e^{j\omega T})|^2 = \frac{(a_o+\sum_{h=1}^{k} \cos n\omega T)^2 + (\sum_{n=1}^{k} a_n \sin n\omega T)^2}{(b_o+\sum_{h=1}^{m} \cos n\omega T)^2 + (\sum_{n=1}^{m} b_n \sin n\omega T)^2} \tag{4.40}$$

which can be reduced to the form

$$|H(e^{j\omega T})|^2 = \frac{\sum_{n=0}^{k} a_n^2 + 2\sum_{n=0}^{k-1} a_n a_{n+1} \cos \omega T + 2\sum_{n=0}^{k-2} a_n a_{n+2} \cos 2\omega T + \ldots}{\sum_{n=0}^{m} b_n^2 + 2\sum_{n=0}^{m-1} b_n b_{n+1} \cos \omega T + 2\sum_{n=0}^{m-2} b_n b_{n+2} \cos 2\omega T + \ldots} \tag{4.41}$$

$$|H(e^{j\omega T})|^2 = \frac{\sum_{n=0}^{k} c_n \cos n\omega T}{\sum_{n=0}^{m} d_n \cos n\omega T} \tag{4.42}$$

Proof of Eq. (4.41) is given in Appendix A. Equation (4.41) indicates that the magnitude squared frequency spectrum is the ratio of two finite Fourier series with cosine terms only. Equation (4.42) shows the relationships between the coefficients of the Fourier series, c_n and d_n and the coefficients of the filter a_j and b_i. Thus, from (4.22) and (4.23)

$$c_n = 2 \sum_{j=0}^{k-n} a_j \, a_{j+n} \tag{4.43a}$$

$$d_n = 2 \sum_{j=0}^{m-n} b_j \, b_{j+n} \tag{4.43b}$$

This relationship can be written in matrix form as follows

$$\begin{bmatrix} a_0 & a_1 & a_2 & \cdots\cdots & a_k \\ 0 & a_0 & a_1 & \cdots\cdots & a_{k-1} \\ 0 & 0 & a_0 & \cdots\cdots & a_{k-2} \\ \vdots & \vdots & \vdots & & \vdots \\ 0 & 0 & 0 & \cdots\cdots & a_0 \end{bmatrix} \begin{bmatrix} a_0 \\ a_1 \\ a_2 \\ \vdots \\ a_k \end{bmatrix} = \begin{bmatrix} c_0 \\ c_{1/2} \\ c_{2/2} \\ \vdots \\ c_{k/2} \end{bmatrix} \tag{4.44}$$

Similar relationships hold for the denominator coefficients. As discussed in the previous section, it is possible to find an approximation to an even function as a rational expression of Fourier series so that c_n and d_n are known. The coefficients of the Fourier series, and hence the vector of c's in Eq. (4.44), will be obtained from the expansion of the desired spectrum function. Solving for the a's in Eq. (4.44) yields the coefficients of the numerator of the digital filter realization. An identical procedure can be followed for the coefficients of the denominator.

This set of nonlinear equations has several solutions, in fact, as k gets larger, the number of solutions also increases. This is not surprising because of the nature of the

problem. That is, given a filter, a unique magnitude squared frequency spectrum function can be found, but the inverse procedure is not unique. Given the magnitude of the spectrum, the description of the filter is incomplete because there is no information about the phase characteristics.

Consider an example of the use of this synthesis method to approximate a given magnitude squared function. For comparison with the example given the same magnitude spectrum shown in Fig. 4.3 will be squared. What results in the same function, which is now approximated with a filter using only two delays for the output and input signals. The nonlinear equations to be solved are of the form

$$a_0^2 + a_1^2 + a_2^2 = c_0 \tag{4.45}$$

$$a_0 a_1 + a_1 a_2 = c_{1/2} \tag{4.46}$$

$$a_s a_2 = c_{2/2} \tag{4.47}$$

Solving this equations algebraically yields

$$a_1 = \pm \sqrt{\frac{c_o + c_2 \pm \sqrt{(c_o + c_2)^2 - c_1^2}}{2}} \tag{4.48}$$

$$a_0 = \frac{c_1}{4a_1} \pm \sqrt{\left(\frac{c_1}{4a_1}\right)^2 - \frac{c_2}{2}} \tag{4.49}$$

$$a_2 = \frac{c_2}{2a_0} \tag{4.50}$$

Equation (4.48) indicates there are four solutions for a_1 and Eq. (4.49) indicates there are two solutions of a_0 for each a_1. Hence there are eight sets of coefficients satisfying the given nonlinear equations. The same is true for the denominator set of coefficients and therefore there are 64 solutions for the filter. In general not all the solution may be valid if only real coefficients are being considered.

Using the results obtained in previous example, Eq. (4.34), the magnitude squared function is expanded in the same ratio of Fourier series, yielding

$$|H(e^{j\omega T})|^2 = \frac{0.01823 + 0.02418 \cos \omega T + 0.00639 \cos 2\omega T}{1.23870 - 1.39494 \cos \omega T + 0.23870 \cos 2\omega T} \quad (4.51)$$

Substituting these coefficients into (4.48), (4.49), (4.50), two sets of solutions are obtained, called filter A and B respectively.

	FILTER A	FILTER B
a_0 =	0.038983093	0.081958605
a_1 =	0.099965521	0.099965521
a_2 =	0.081958605	0.038983093
b_0 =	-0.284898296	-0.418921424
b_1 =	0.990978207	0.990978207
b_2 =	-0.418921424	-0.284898296

The magnitude and phase versus frequency characteristics are shown in Fig. 4.11, 4.12, 4.13, 4.14.

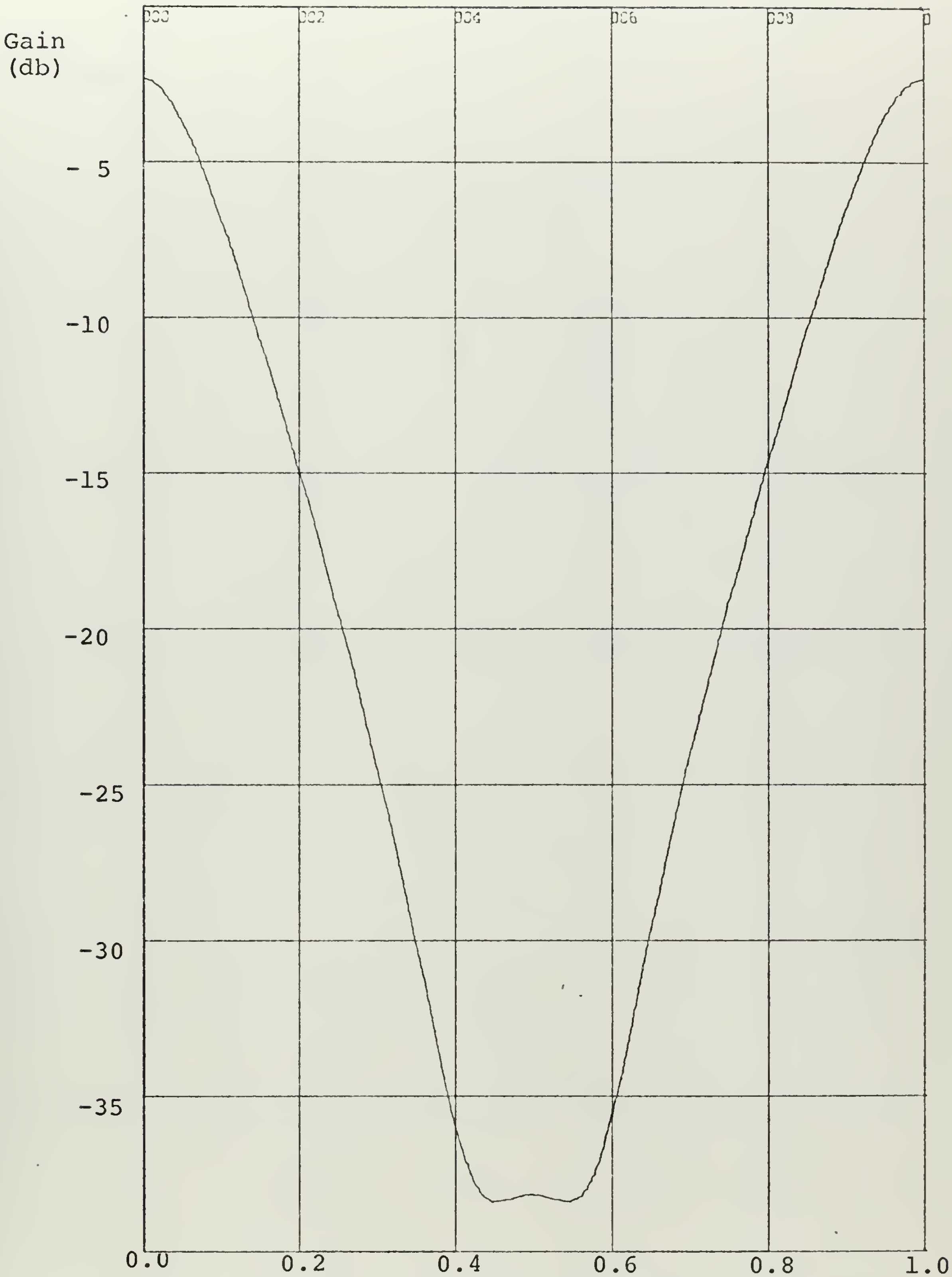

Fig. 4.11 Magnitude vs. normalized frequency. Recursive filter, coefficients obtained from magnitdue squared criterion. Filter A.

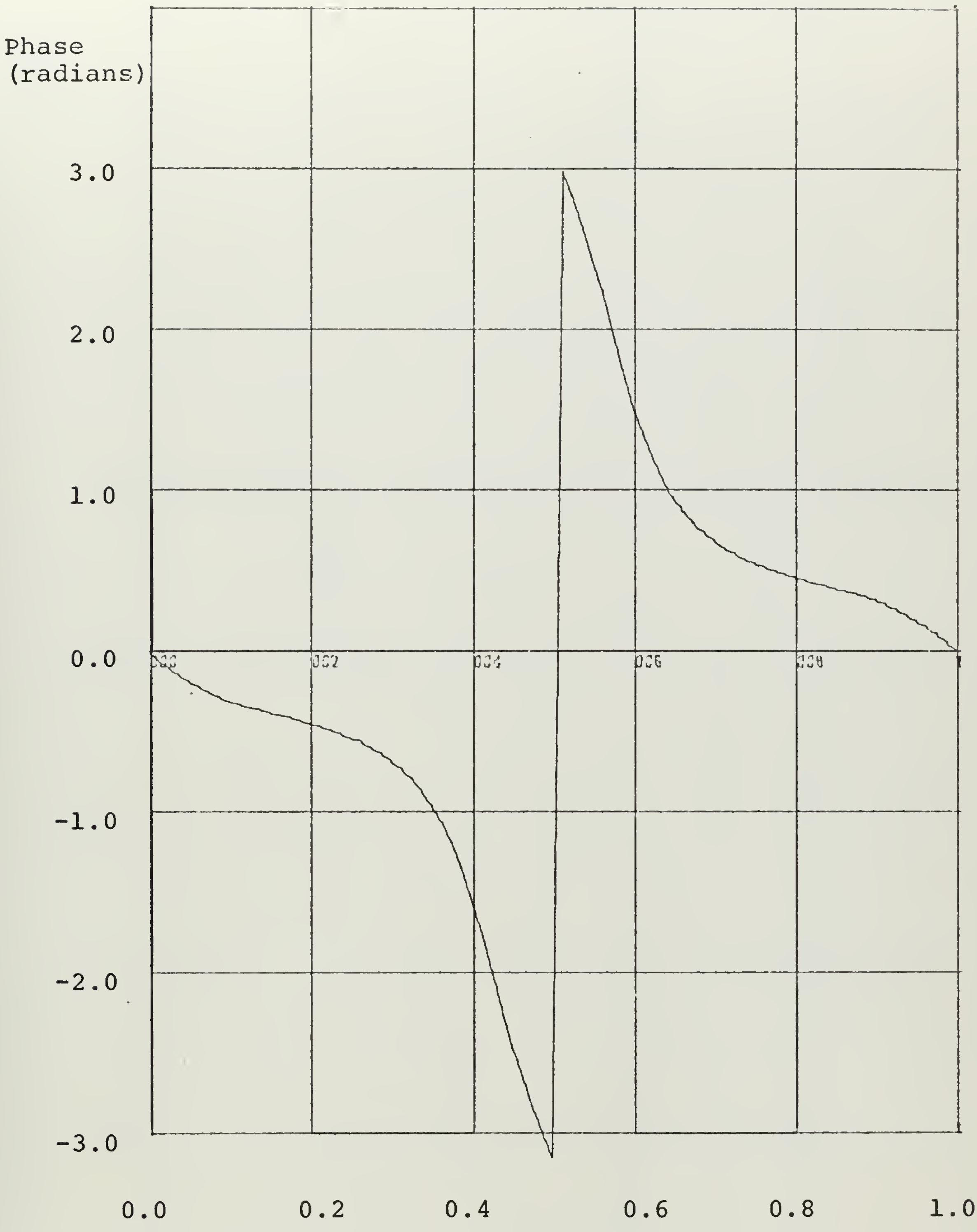

Fig. 4.12 Phase vs. normalized frequency. Recursive filter, coefficients obtained from magnitude squared criterion. Filter A.

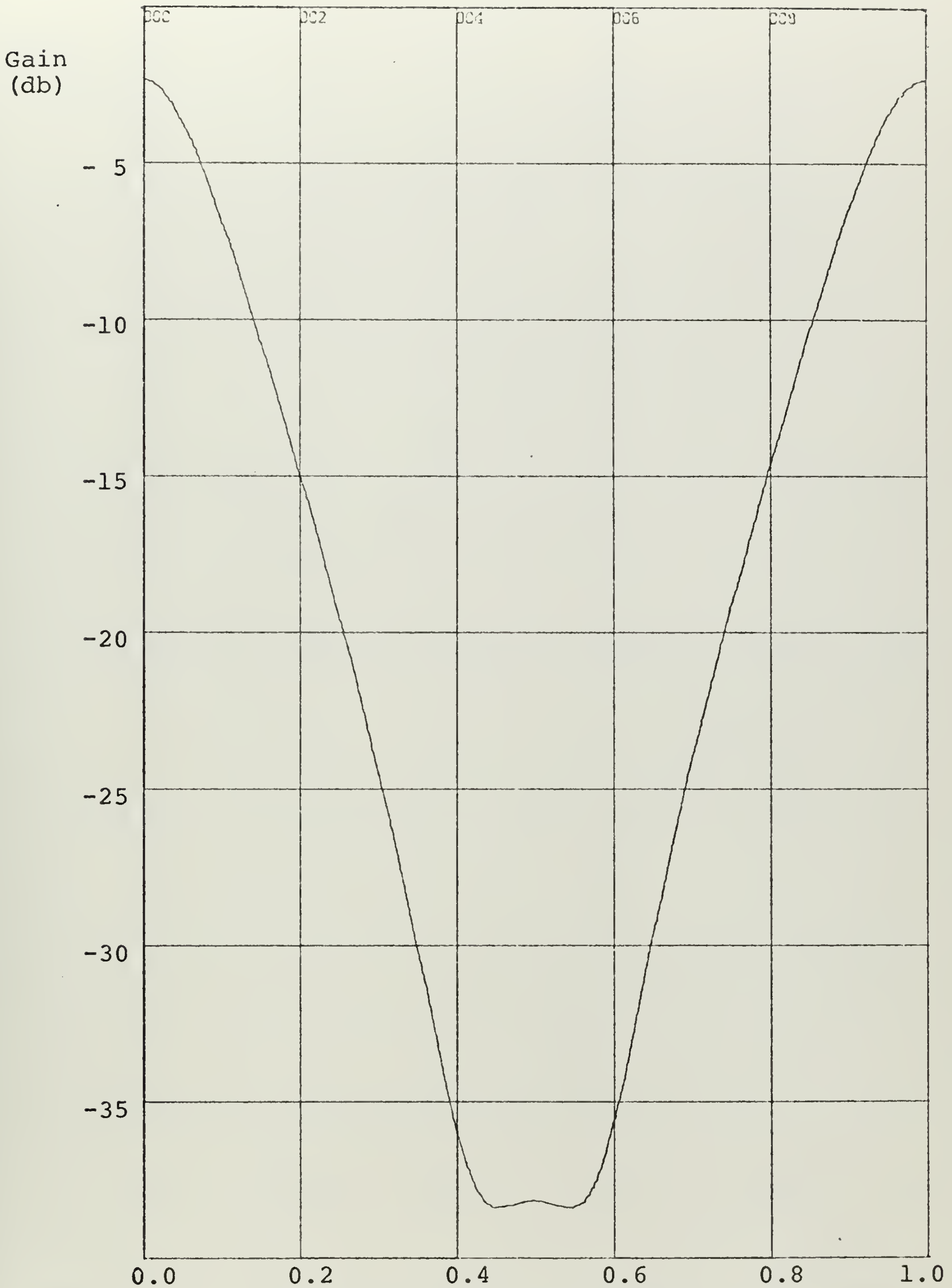

Fig. 4.13 Magnitude vs. normalized frequency. Recursive filter, coefficients obtained from magnitude squared criterion. Filter B.

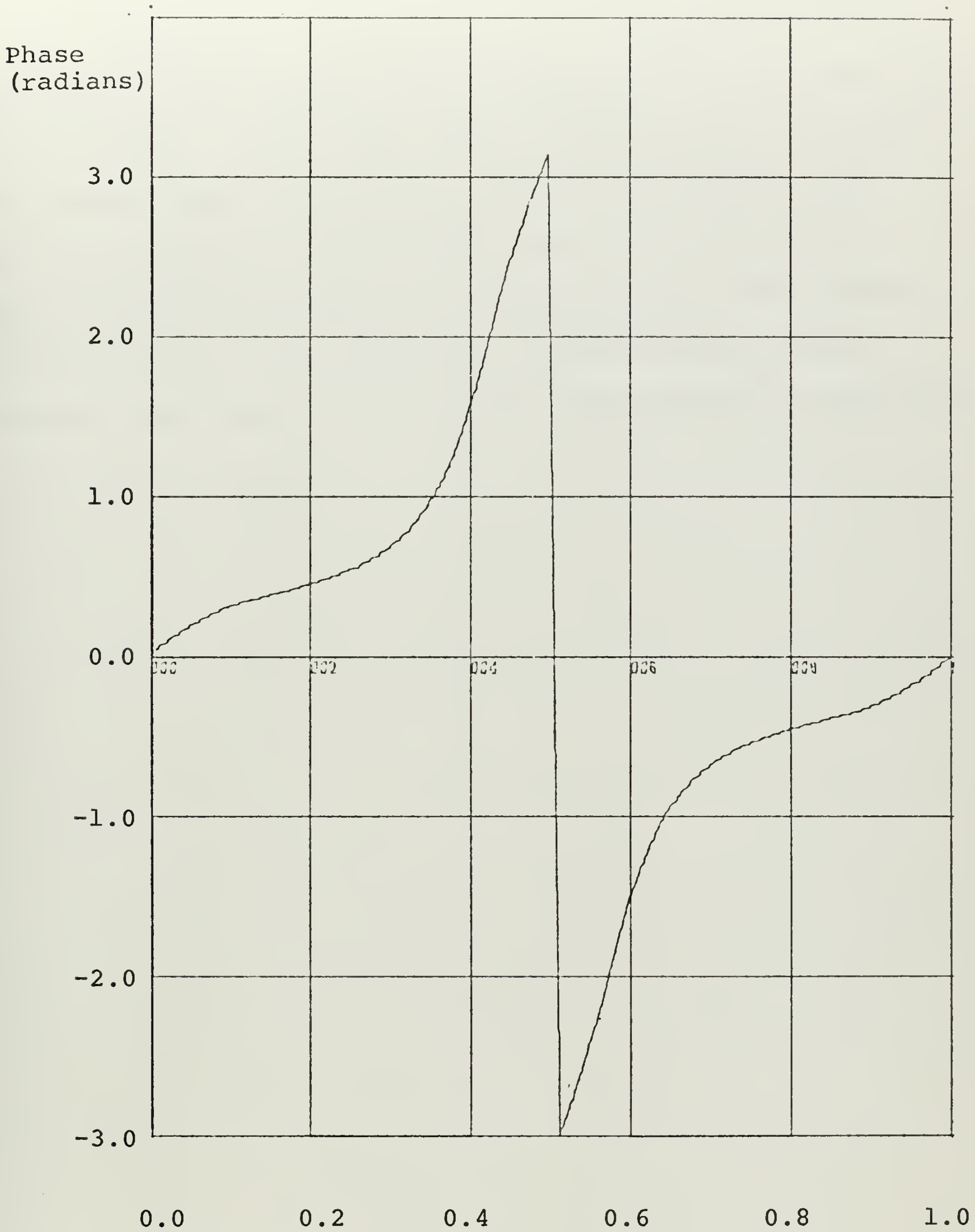

Fig. 4.14 Phase vs. normalized frequency. Recursive filter, coefficients obtained from magnitude squared criterion. Filter B.

Comparison of filters A and B indicates the same magnitude for both filters and a different phase characteristic as was expected. With these sets of coefficients, still two more combinations are possible, that is the numerator of A and the denominator of B and vice versa. At this point, nothing has been said about the phase characteristic of this synthesis method. It is left as a suggestion for further research, the introduction of phase characteristics restrictions.

V. SUMMARY AND SUGGESTIONS FOR FURTHER RESEARCH

The two main new ideas introduced in the thesis are:

1. A generalization of Martin's synthesis technique to include recursive filters, which allows filters with zero phase or linear phase characteristics, to be obtained.

2. A new synthesis technique, which depends upon the expansion of a given function as a ratio of two Fourier series. The resulting technique involves the solution of simultaneous nonlinear algebraic equations, but the filter requires half the storage of Martin's method for the same degree of approximation. The number of multiplications to be performed is also decreased by one half.

The foregoing studies have given rise to several basic questions for further research:

1. Explore the concept of expanding a given function as a ratio of two finite Fourier series directly from Fourier series expansion theory, as versus the change of variable technique, involving Chebyshev polynomials, developed in this thesis. It would appear that an unlimited number of ratios are possible. If this is the case, filter stability can be assured by selecting the poles of the digital transfer function to lie inside the unit circle of the z plane, and then selecting the coefficients of the numerator to obtain the desired magnitude spectrum.

2. Consider synthesis procedures starting from a classical specification for the filter in terms of tolerance bands and attenuation rates. Determine how these design criteria can be met.

3. Find a general method to solve the nonlinear equations, Eq. (4.44), which were developed for the filter synthesis proceedure starting from a magnitude squared function as discussed.

Appendix A

Derivation of Equation (4.22)

$$|H(e^{j\omega T})|^2 = \frac{(a_0 + \sum_{n=1}^{k} a_n \cos n\omega T)^2 + (\sum_{n=1}^{k} a_n \sin n\omega T)^2}{b_0 + \sum_{n=1}^{k} b_n \cos n\omega T)^2 + (\sum_{n=1}^{k} a_m \sin m\omega T)^2} \qquad (A.1)$$

consider the numerator only

$$|N(\omega T)|^2 = a_0 + \sum_{n=1}^{k} a_n \cos n\omega T)^2 + (\sum_{n=1}^{k} a_n \sin n\omega T)^2$$

$$= a_0^2 + 2a_0 \sum_{n=1}^{k} a_n \cos n\omega T + (\sum_{n=1}^{k} a_n \cos n\omega T)^2 + (\sum_{n=1}^{k} a_n \sin n\omega T)^2 \qquad (A.2)$$

The last two terms can be expanded as follows:

$$(\sum_{n=1}^{k} a_n \cos n\omega T)^2 + (\sum_{n=1}^{k} a_n \sin n\omega T)^2 = \sum_{n=1}^{k} a_n^2 \cos^2 n\omega T$$

$$+ 2\sum_{n=1}^{k-1} a_n \cos n\omega T \sum_{j=n+1}^{k} a_j \cos j\omega T + \sum_{n=1}^{k} a_n^2 \sin^2 n\omega T$$

$$+ 2\sum_{n=1}^{k-1} a_n \sin n\omega T \sum_{j=n+1}^{k} a_j \sin j\omega T \qquad (A.3)$$

$$= \sum_{n=1}^{k} a_n^2 (\cos^2 n\omega T + \sin^2 m\omega T) + 2\sum_{n=1}^{k-1} a_n \Big\{\cos n\omega T \sum_{j=n+1}^{k} a_j \cos j\omega T$$

$$+ \sin n\omega T \sum_{n=n+1}^{k} a_j \sin j\omega T\Big\} \qquad (A.4)$$

$$= \sum_{n=1}^{k} a_n^2 + 2 \sum_{n=1}^{k-1} \left\{ \sum_{j=n+1}^{k} a_n \cos n\omega T \, a_j \cos j\omega T \right.$$

$$\left. + \sum_{n=n+1}^{k} a_n \cos n\omega T \, a_j \sin j\omega T \right\} \qquad (A.5)$$

$$= \sum_{n=1}^{k} a_n^2 + 2 \sum_{n=1}^{k-1} \left\{ \sum_{j=n+1}^{k} a_n a_j \{\cos n\omega T \cos j\omega T \right.$$

$$\left. + \sin n\omega T \sin j\omega T\} \right\} \qquad (A.6)$$

Use the trigonometric identity

$$\{\cos n\omega T \cos j\omega T + \sin n\omega T \sin j\omega T\} = \cos (j-n)\omega T \qquad (A.7)$$

$$= \sum_{i=1}^{k} a_n^2 + 2 \sum_{n=1}^{k-1} \left\{ \sum_{j=n+1}^{k} a_n a_j \cos (j-n)\omega T \right\}$$

changing subscripts, $i = j-n$, $j = n+i$ the limits of the second summation become

$$j = n+1 \quad \rightarrow \quad i = 1$$

$$j = k \quad \rightarrow \quad i = k-n$$

$$= \sum_{n=1}^{k} a_n^2 + 2 \sum_{n=1}^{k-1} \sum_{i=1}^{k-n} a_n a_{n+i} \cos i \, \omega T \qquad (A.8)$$

Changing summation order Eq. (A.8) becomes

$$= \sum_{n=1}^{k} a_n^2 + 2 \sum_{i=1}^{k-1} \left\{ \sum_{n=1}^{K-i} a_n a_{n+i} \right\} \cos i \, \omega T \qquad (A.9)$$

Combining (A.9) with (A.2) yields

$$|N(\omega T)|^2 = a_0^2 + 2 \sum_{i=1}^{k} a_0 a_{0+i} \cos i\,\omega T + \sum_{n=1}^{k} a_n^2$$

$$+ 2 \sum_{i=1}^{k-1} \sum_{n=1}^{k-1} a_n a_{n+i} \cos i\,\omega T \qquad (A.10)$$

$$= \sum_{n=0}^{k} a_n^2 + 2\, a_0 a_k \cos k\,\omega T + 2 \sum_{i=1}^{k-1} a_0 a_{0+i} \cos i\,\omega T$$

$$+ 2 \sum_{i-1}^{k-1} \sum_{n=1}^{k-1} a_n a_{n+i} \cos i\,\omega T \qquad (A.11)$$

$$= \sum_{n=0}^{k} a_n^2 + 2\, a_0 a_k \cos k\,\omega T + 2 \sum_{i=1}^{k-1} \sum_{n=0}^{k-i} a_n a_{n+i} \cos i\,\omega T \qquad (A.12)$$

$$= \sum_{n=0}^{k} a_n^2 + 2 \sum_{i=1}^{k} \sum_{n=0}^{k-1} a_n a_{n+i} \cos i\,\omega T \qquad (A.13)$$

The same relationship holds for the denominator, and so established the validity of Eq. (4.22).

LIST OF REFERENCES

1. Ragazzini, J., Zadah, L. H., "The Analysis of Sampled-Data System," A.I.E.E. Transactions, V.71, Part II, pp 225-234, 1952.

2. Kuo, B. C., Analysis and Synthesis of Sampled-Data Control Systems, pp 54-103, Prentice-Hall, 1963.

3. Salzer, J. M., "Frequency Analysis of Digital Computers Operating in Real Time," Proceedings of the I.R.E., pp 457-466, February 1954.

4. Tustin, A., "A Method of Analyzing the Behavior of Linear Systems in Terms of Time Series," Journal I.E.E., V.94, Part II A, pp 130-142, May 1947.

5. New York University Report 400-99, The General Theory of Digital Filters with Applications to Spectral Analysis, by K. Steiglitz, p 57, May 1963.

6. Martin, M. A., "Frequency Domain Applications to Data Processing," I.R.E. Transactions on Space Electronics and Telemetry, V. SET 5, No.1, pp 33-41, March 1959.

7. DeRusso, P. M., Roy, R. J., Close, C. M., State Variables for Engineers, pp 6-8, Wiley, 1965.

8. Oliver, R. M., Pierce, J. R., Shannon, C. E., "The Philosophy of Pulse Code Modulation," Proceedings I.R.E., V.36, No.11, pp 1324-1331, November 1948.

9. Fogel, L. J., "A Note on the Sampling Theorem," I.R.E. Transactions on Information Theory, pp 47-48, March 1955.

10. Greaves, C. J., Cadzow, J. A., "The Optimal Discrete Filter Corresponding To a Given Analog Filter," I.E.E.E. Transactions on Automatic Control, V.12, p 306, June 1967.

11. Sage, A. P., Burt, R. W., "Optimum Design and Error Analysis of Digital Integrators for Discrete System Simulation," Proceedings Fall Joint Computer Conference, pp 903-914, 1965.

12. Hamming, R. W., Numerical Methods for Scientist and Engineers, pp 293-300, McGraw-Hill, 1962.

13. Hamming, R. W., Op. cited, pp 249-251.

14. McCracken, D. D. Dorn W. S., Numerical Methods and Fortran Programming, p 416, Wiley, 1964.

15. Gold, B., Rader, C. M., Digital Processing of Signals, pp 70-78, McGraw-Hill, 1969.

INITIAL DISTRIBUTION LIST

		No. Copies
1.	Defense Documentation Center Cameron Station Alexandria, Virginia 22314	2
2.	Library, Code 0212 Naval Postgraduate School Monterey, California 93940	2
3.	Assoc. Professor G. E. Subak-Sharpe 606 We. 116th Street, Apt. 71 New York, New York 10027	1
4.	Professor S. R. Parker, Code 52Px Department of Electrical Engineering Naval Postgraduate School Monterey, California 93940	1
5.	LT(jg) A. Partarrieu Casilla 5112 Santiago Chile	1
6.	Director de Armamentos de la Armada Correo Naval Valparaiso Chile	1
7.	Director de Instrucción de la Armada Correo Naval Valparaiso Chile	1
8.	Director de la Escuela Naval Correo Naval Valparaiso Chile	1

Security Classification

DOCUMENT CONTROL DATA - R & D

(Security classification of title, body of abstract and indexing annotation must be entered when the overall report is classified)

1. ORIGINATING ACTIVITY (Corporate author) Naval Postgraduate School Monterey, California 93940	2a. REPORT SECURITY CLASSIFICATION Unclassified 2b. GROUP

3. REPORT TITLE

Synthesis of Digital Filters from Frequency Spectrum Characteristics

4. DESCRIPTIVE NOTES (Type of report and, inclusive dates)

Master's Thesis and Electrical Engineer; September 1970

5. AUTHOR(S) (First name, middle initial, last name)

Arthur Laurent Partarrieu

6. REPORT DATE	7a. TOTAL NO. OF PAGES	7b. NO. OF REFS
September 1970	96	15

8a. CONTRACT OR GRANT NO.	9a. ORIGINATOR'S REPORT NUMBER(S)
b. PROJECT NO.	
c.	9b. OTHER REPORT NO(S) (Any other numbers that may be assigned this report)
d.	

10. DISTRIBUTION STATEMENT

This document has been approved for public release and sale; its distribution is unlimited.

11. SUPPLEMENTARY NOTES	12. SPONSORING MILITARY ACTIVITY
	Naval Postgraduate School Monterey, California 93940

13. ABSTRACT

A comparison of standard z transform and algebraic substitution synthesis methods for digital filters are presented with emphasis on the frequency domain characteristics. A generalization of Martin's procedure, which leads to recursive filters, is obtained. Also a new method to synthesize a digital filter from a magnitude squared versus frequency characteristic specification is presented.

DD FORM 1 NOV 65 1473 (PAGE 1)

S/N 0101-807-6811

Security Classification

A-31408

Security Classification

14 KEY WORDS	LINK A		LINK B		LINK C	
	ROLE	WT	ROLE	WT	ROLE	WT
Digital filters						
Discrete time filter synthesis						

DD FORM 1 NOV 65 1473 (BACK)

S/N 0101-807-6821

Security Classification

A-31409

Thesis 125880
P22 Partarrieu
c.1 Synthesis of digital filters from frequency spectrum characteristics.